

Supplementary Information for: Population-specific  
causal disease effect sizes in functionally important  
regions impacted by selection

# 1 Supplementary notes

## 2 Causal and joint-fit effect size

3 Following ref,<sup>1</sup> we define causal effect size of a SNP as the underlying *true* effect size of  
4 the SNP on phenotype; we define joint-fit effect size of a SNP as the *inferred* effect size of  
5 the SNP. Causal effect size of a SNP is unique, whereas joint-fit effect size is subjected to  
6 the set of SNPs included in fitting the model for inferring the causal effect. Previous work<sup>2</sup>  
7 estimates trans-ethnic genetic correlation of joint-fit effect size – the set of SNPs for model  
8 fitting is the set of SNPs with minor allele frequency greater than 5% in both populations.<sup>1,2</sup>  
9 In this work, we focus on estimating trans-ethnic genetic correlation of causal effect size.

## 10 Per-allele and standardized causal effect size

11 Per-allele causal effect size of a SNP is the change in phenotype resulted from having  
12 an additional allele at that SNP. Standardized causal effect size of a SNP is the change in  
13 phenotype per standard deviation increase in normalized genotype of that SNP. Per-allele  
14 and standardized causal effect size of a SNP are related to each other through

$$\beta_{\text{standardized}} = \sqrt{2p(1-p)}\beta_{\text{per-allele}}, \quad (1)$$

15 where  $p$  is the minor allele frequency (MAF) of the SNP in a population. Comparing stan-  
16 dardized causal effect size of a SNP across populations is less informative due to differences  
17 in MAF. Thus, we focus on comparing per-allele causal effect size across populations in this  
18 work.

## 19 Defining stratified squared trans-ethnic genetic correlation of per- 20 allele causal effect size

21 We model a complex phenotype in two populations using linear models,

$$\begin{aligned} \mathbf{Y}_1 &= \mathbf{X}_1\boldsymbol{\beta}_1 + \boldsymbol{\epsilon}_1, \\ \mathbf{Y}_2 &= \mathbf{X}_2\boldsymbol{\beta}_2 + \boldsymbol{\epsilon}_2, \end{aligned} \quad (2)$$

22 where  $\mathbf{Y}_1 \in \mathbb{R}^{N_1}$  and  $\mathbf{Y}_2 \in \mathbb{R}^{N_2}$  are vectors of standardized phenotype measurements with 0  
23 mean and unit variance in the two populations, with sample size  $N_1$  and  $N_2$ , respectively;  
24  $\mathbf{X}_1 \in \mathbb{R}^{N_1 \times M}$  and  $\mathbf{X}_2 \in \mathbb{R}^{N_2 \times M}$  are mean centered (but *not normalized*) genotype matrices of  
25 the two populations across  $M$  SNPs, respectively;  $\boldsymbol{\beta}_1 \in \mathbb{R}^M$  and  $\boldsymbol{\beta}_2 \in \mathbb{R}^M$  are the *per-allele*

26 *causal* effect size vectors of the  $M$  SNPs on phenotypes in the two populations, respectively;  
 27 and  $\mathbf{e}_1 \in \mathbb{R}^{N_1}$  and  $\mathbf{e}_2 \in \mathbb{R}^{N_2}$  are the environmental effects in the two populations, respectively.  
 28 We model per-allele causal effect sizes, instead of standardized effect sizes as is modeled in  
 29 LDSC, to account for differences in minor allele frequency across different populations.

30 We assume both  $\mathbf{X}_1$  and  $\mathbf{X}_2$  to be random. We assume a random effect model for the  
 31 per-allele causal effect sizes of SNP  $j$  in the two populations,  $\beta_{1j}$  and  $\beta_{2j}$ , respectively, with  
 32 mean, variance, and covariance,

$$\begin{aligned} \mathbb{E}[\beta_{1j}] &= 0, \text{Var}[\beta_{1j}] = \sum_C a_j(C) \tau_{1C}, \\ \mathbb{E}[\beta_{2j}] &= 0, \text{Var}[\beta_{2j}] = \sum_C a_j(C) \tau_{2C}, \\ \text{Cov}[\beta_{1j}, \beta_{2j}] &= \sum_C a_j(C) \theta_C, \end{aligned} \tag{3}$$

33 where  $a_j(C)$  is SNP  $j$ 's value with respect to annotation  $C$ ;  $\tau_{1C}$  and  $\tau_{2C}$  are the net contri-  
 34 bution of annotation  $C$  to the variance of per-allele causal effect size of SNP  $j$  in the two  
 35 populations;  $\theta_C$  the net contribution of annotation  $C$  to the co-variance of per-allele causal  
 36 effect size of SNP  $j$  in the two populations.

37 We define stratified trans-ethnic genetic co-variance of a binary annotation  $C$  (e.g.  
 38 functional annotations or quintiles of continuous-valued annotations) as the sum of per-SNP  
 39 genetic covariance of SNPs that are a member of annotation  $C$ ,

$$\rho_g(C) = \sum_{j \in C} \text{Cov}[\beta_{1j}, \beta_{2j}] = \sum_{j \in C} \sum_{C'} a_j(C') \theta_{C'}. \tag{4}$$

40 Here,  $C$  is a binary annotation, but  $C'$  can be either binary or continuous-valued. Similarly,  
 41 we define stratified heritability (of *per-allele* causal effect sizes) of a binary annotation  $C$  in  
 42 the two populations as,

$$\begin{aligned} h_{g1}^2(C) &= \sum_{j \in C} \text{Var}[\beta_{1j}] = \sum_{j \in C} \sum_{C'} a_j(C') \tau_{1C'}, \\ h_{g2}^2(C) &= \sum_{j \in C} \text{Var}[\beta_{2j}] = \sum_{j \in C} \sum_{C'} a_j(C') \tau_{2C'}. \end{aligned} \tag{5}$$

43 We define stratified trans-ethnic genetic correlation as

$$r_g(C) = \frac{\rho_g(C)}{\sqrt{h_{g1}^2(C) h_{g2}^2(C)}}. \tag{6}$$

44 Since estimates of  $h_{g1}^2(C)$  and  $h_{g2}^2(C)$  can be noisy and possibly negative, rendering the square  
 45 roots undefined, we estimate stratified squared trans-ethnic genetic correlation instead, which  
 46 is defined as,

$$r_g^2(C) = \frac{\rho_g^2(C)}{h_{g1}^2(C)h_{g2}^2(C)}. \quad (7)$$

47 Another advantage of estimating  $r_g^2(C)$  over  $r_g(C)$  is that taking square root of a random  
 48 variable creates downward bias, which is difficult to correct for – estimating  $r_g^2(C)$  resolves  
 49 this issues. In this work, we only estimate  $r_g^2(C)$  for SNPs with minor allele frequency (MAF)  
 50 greater than 5% in both populations. Additionally, we define enrichment of stratified squared  
 51 trans-ethnic genetic correlation,

$$\lambda^2(C) = \frac{r_g^2(C)}{r_g^2}, \quad (8)$$

52 as the ratio between stratified squared trans-ethnic genetic correlation of annotation  $C$  and  
 53 squared genome-wide trans-ethnic genetic correlation; we meta-analyze  $\lambda^2(C)$  across different  
 54 traits.

## 55 **Estimating stratified squared trans-ethnic genetic correlation**

### 56 **Regression equations to estimate $\theta_C$ and $\tau_C$**

57 We estimate the net contributions of annotation to per-SNP trans-ethnic genetic co-  
 58 variance and per-allele heritability,  $\theta_C$ ,  $\tau_{1C}$  and  $\tau_{2C}$ , respectively, from GWAS summary  
 59 association statistics using methods of moments.

60 In genome-wide association studies (GWAS) across two populations, Z-scores testing  
 61 association between SNP  $j$  and the trait are calculated as,

$$\begin{aligned} Z_{1j} &= \frac{1}{\sigma_{1j}\sqrt{N_1}} \mathbf{X}_{1j}^T \mathbf{Y}_1, \\ Z_{2j} &= \frac{1}{\sigma_{2j}\sqrt{N_2}} \mathbf{X}_{2j}^T \mathbf{Y}_2. \end{aligned} \quad (9)$$

62 where  $Z_{1j}$  and  $Z_{2j}$  are Z-scores for SNP  $j$  in the two populations, respectively;  $\sigma_{1j}$  and  $\sigma_{2j}$   
 63 are the standard deviation of SNP  $j$  in the two population.

Substituting the linear phenotype model from Equation (2), it can be shown that

$$\begin{aligned}
\mathbb{E}[Z_{1j}Z_{2j}] &= \frac{1}{\sigma_{1j}\sigma_{2j}\sqrt{N_1N_2}} \mathbb{E} \left[ (\mathbf{X}_{1j}^\top \mathbf{X}_1 \boldsymbol{\beta}_1 + \mathbf{X}_{1j}^\top \boldsymbol{\epsilon}_1) (\mathbf{X}_{2j}^\top \mathbf{X}_2 \boldsymbol{\beta}_2 + \mathbf{X}_{2j}^\top \boldsymbol{\epsilon}_2) \right] \\
&= \frac{1}{\sigma_{1j}\sigma_{2j}\sqrt{N_1N_2}} \mathbb{E} \left[ \left( \mathbf{X}_{1j}^\top \left( \sum_{k=1}^M \mathbf{X}_{1k} \beta_{1k} \right) \right) \left( \mathbf{X}_{2j}^\top \left( \sum_{k=1}^M \mathbf{X}_{2k} \beta_{2k} \right) \right) \right] \\
&= \frac{1}{\sigma_{1j}\sigma_{2j}\sqrt{N_1N_2}} \mathbb{E} \left[ \left( \sum_{k=1}^M \beta_{1k} \mathbf{X}_{1j}^\top \mathbf{X}_{1k} \right) \left( \sum_{k=1}^M \beta_{2k} \mathbf{X}_{2j}^\top \mathbf{X}_{2k} \right) \right] \\
&= \frac{1}{\sigma_{1j}\sigma_{2j}\sqrt{N_1N_2}} \mathbb{E} \left[ \sum_{k=1}^M \beta_{1k} \beta_{2k} (\mathbf{X}_{1j}^\top \mathbf{X}_{1k}) (\mathbf{X}_{2j}^\top \mathbf{X}_{2k}) \right] \tag{10} \\
&= \frac{1}{\sigma_{1j}\sigma_{2j}\sqrt{N_1N_2}} \sum_{k=1}^M \text{Cov}[\beta_{1k}, \beta_{2k}] \mathbb{E}[\mathbf{X}_{1j}^\top \mathbf{X}_{1k}] \mathbb{E}[\mathbf{X}_{2j}^\top \mathbf{X}_{2k}] \\
&= \frac{1}{\sigma_{1j}\sigma_{2j}\sqrt{N_1N_2}} \sum_{k=1}^M \sum_C \theta_C a_k(C) N_1 \rho_{1jk} N_2 \rho_{2jk} \\
&= \sqrt{N_1 N_2} \sum_C \left( \sum_{k=1}^M \frac{\rho_{1jk} \rho_{2jk}}{\sigma_{1j} \sigma_{2j}} a_k(C) \right) \theta_C,
\end{aligned}$$

where  $\rho_{1jk}$  and  $\rho_{2jk}$  are the covariances between SNP  $j$  and  $k$  in population 1 and population 2, respectively. Let

$$\ell_x(j, C) = \sum_{k=1}^M \frac{\rho_{1jk} \rho_{2jk}}{\sigma_{1j} \sigma_{2j}} a_k(C) \tag{11}$$

be the trans-ethnic LD score of SNP  $j$  with respect to annotation  $C$ , we arrive at the regression equation for estimating  $\theta_C$ ,

$$\mathbb{E}[Z_{1j}Z_{2j} | \ell_x(j, C)] = \sqrt{N_1 N_2} \sum_C \ell_x(j, C) \theta_C. \tag{12}$$

Following ref.<sup>3</sup>, regression equations for estimating  $\tau_{1C}$  and  $\tau_{2C}$ , contribution of annotation  $C$  to per-SNP heritability, can be derived similarly,

$$\begin{aligned}
\mathbb{E}[\chi_{1j}^2 | \ell_1(j, C)] &= N_1 \sum_C \ell_1(j, C) \tau_{1C} + N_1 a_1 + 1, \\
\mathbb{E}[\chi_{2j}^2 | \ell_2(j, C)] &= N_2 \sum_C \ell_2(j, C) \tau_{2C} + N_2 a_2 + 1,
\end{aligned} \tag{13}$$

where

$$\ell_p(j, C) = \sum_{k=1}^M \frac{\rho_{pj}^2}{\sigma_{pj}^2} a_k(C) \tag{14}$$

72 is the LD score of SNP  $j$  with respect to annotation  $C$  in population  $p$ ; and  $a_p$  is the intercept  
73 term capturing population stratification in population  $p$ . An intercept term is not necessary  
74 in the regression in Equation (12), as GWAS from different populations are not expected to  
75 share samples or shared population stratification.

## 76 Estimating LD scores

77 We estimate trans-ethnic and population-specific LD scores using publicly available  
78 reference genotypes of 481 East Asian and 489 European individuals from the 1000 Genomes  
79 Project.<sup>4</sup>

80 Let  $\mathbf{X}_1 \in \mathbb{R}^{N_1 \times M}$  and  $\mathbf{X}_2 \in \mathbb{R}^{N_2 \times M}$  be the mean centered (but *not normalized*) reference  
81 genotype matrices for  $M$  SNPs in the two populations, with reference sample size  $N_1$  and  $N_2$ ,  
82 respectively, we obtain unbiased estimates of trans-ethnic LD score of SNP  $j$  with respect  
83 to annotation  $C$ ,  $\ell_\times(j, C)$  as

$$\hat{\ell}_\times(j, C) = \frac{1}{\hat{\sigma}_{1j}\hat{\sigma}_{2j}} \sum_{k=1}^M \hat{\rho}_{1jk}\hat{\rho}_{2jk}, \quad (15)$$

84 where

$$\hat{\rho}_{pj k} = \frac{\mathbf{X}_{pk}^\top \mathbf{X}_{pj}}{N_p - 1}, \quad \hat{\sigma}_{pj}^2 = \frac{\mathbf{X}_{pj}^\top \mathbf{X}_{pj}}{N_p - 1}. \quad (16)$$

85 At sample size of  $N_1 = 481$  and  $N_2 = 489$ , both standard deviation estimation and ratio  
86 estimation are nearly unbiased. Thus, to show  $\mathbb{E}[\hat{\ell}_\times(j, C)] = \ell_\times(j, C)$ , it suffices to show  
87  $\mathbb{E}[\hat{\rho}_{1jk}\hat{\rho}_{2jk}] = \rho_{1jk}\rho_{2jk}$ . Indeed,

$$\begin{aligned} \mathbb{E}[\hat{\rho}_{1jk}\hat{\rho}_{2jk}] &= \mathbb{E}\left[\left(\frac{\mathbf{X}_{1k}^\top \mathbf{X}_{1j}}{N_1 - 1}\right)\left(\frac{\mathbf{X}_{2k}^\top \mathbf{X}_{2j}}{N_2 - 1}\right)\right] \\ &= \frac{1}{(N_1 - 1)(N_2 - 1)} \mathbb{E}\left[\sum_{i=1}^{N_1} \mathbf{X}_{1ik} \mathbf{X}_{1ij} \sum_{i'=1}^{N_2} \mathbf{X}_{2i'k} \mathbf{X}_{2i'j}\right] \\ &= \frac{1}{(N_1 - 1)(N_2 - 1)} \sum_{i=1}^{N_1} \sum_{i'=1}^{N_2} \mathbb{E}[\mathbf{X}_{1ik} \mathbf{X}_{1ij} \mathbf{X}_{2i'k} \mathbf{X}_{2i'j}] \\ &= \frac{(N_1 - 1)\rho_{1jk}(N_2 - 1)\rho_{2jk}}{(N_1 - 1)(N_2 - 1)} \\ &= \rho_{1jk}\rho_{2jk}, \end{aligned} \quad (17)$$

88 where the equality on the fourth line follows from Isserlis' theorem<sup>5</sup> and the fact that unad-  
89 justed sample covariance is biased by a factor of  $\frac{N-1}{N}$ . When estimating the trans-ethnic LD  
90 scores, we restrict to SNPs that are present in both populations. Effectively, we assume that

91 only SNPs present in both populations contribute to genetic covariance. Since LD is small  
 92 outside a 1 centimorgan window, we only include SNPs within a 1 centimorgan window in  
 93 the summation in Equation (17), similar to previous works.<sup>3,6,7</sup>

94 Similarly, we obtain unbiased estimates of population-specific LD score,  $\ell_p(j, C)$ , as

$$\hat{\ell}_p(j, C) = \frac{1}{\hat{\sigma}_{pj}^2} \sum_{k=1}^M \frac{N_p}{N_p - 1} \left( \hat{\rho}_{pj k}^2 - \frac{\hat{\sigma}_{pj}^2 \hat{\sigma}_{pk}^2}{N_p - 1} \right). \quad (18)$$

95 For sample size of  $N_1 = 481$  and  $N_2 = 489$ , the bias introduced in ratio estimation is  
 96 negligible. Thus, to show  $\hat{\ell}_p(j, C)$  is unbiased, it suffices to show  $E \left[ \hat{\rho}_{pj k}^2 - \frac{\hat{\sigma}_{pj}^2 \hat{\sigma}_{pk}^2}{N_p} \right] = \frac{N_p - 1}{N_p} \rho_{pj k}^2$ .  
 97 Indeed,

$$\begin{aligned} E \left[ \hat{\rho}_{pj k}^2 - \frac{\hat{\sigma}_{pj}^2 \hat{\sigma}_{pk}^2}{N_p} \right] &= E \left[ \left( \frac{\mathbf{X}_{pk}^T \mathbf{X}_{pj}}{N_p - 1} \right)^2 - \frac{\hat{\sigma}_{pj}^2 \hat{\sigma}_{pk}^2}{N_p - 1} \right] \\ &= \left( \frac{1}{N_p - 1} \right)^2 E \left[ \sum_{i=1}^{N_p} \sum_{i'=1}^{N_p} \mathbf{X}_{pi k} \mathbf{X}_{pi j} \mathbf{X}_{pi' k} \mathbf{X}_{pi' j} \right] - \frac{\sigma_{pj}^2 \sigma_{pk}^2}{N_p - 1} \\ &= \left( \frac{1}{N_p - 1} \right)^2 \sum_{i=1}^{N_p} \sum_{i'=1}^{N_p} E [\mathbf{X}_{pi k} \mathbf{X}_{pi j} \mathbf{X}_{pi' k} \mathbf{X}_{pi' j}] - \frac{\sigma_{pj}^2 \sigma_{pk}^2}{N_p - 1} \\ &= \left( \frac{1}{N_p - 1} \right)^2 [(N_p - 1)^2 \rho_{pj k}^2 + (N_p - 1) \sigma_j^2 \sigma_k^2 + (N_p - 1) \rho_{pj k}^2] - \frac{\sigma_{pj}^2 \sigma_{pk}^2}{N_p - 1} \\ &= \frac{N_p - 1}{N_p} \rho_{jk}^2. \end{aligned} \quad (19)$$

98 When estimating the trans-ethnic LD scores, we restrict to SNPs that are present in popu-  
 99 lation  $p$ . Effectively, we assume that SNPs present in population  $p$  contribute to heritability.  
 100 Since LD is small outside a 1 centimorgan window, we only include SNPs within a 1 centi-  
 101 morgan window in the summation for estimating LD scores.

## 102 Regression SNPs and regression weights

103 To mitigate potential confounding due to imputation quality, we include only well-  
 104 imputed SNPs (INFO > 0.9) in the regression. We further restrict to HapMap 3<sup>8</sup> SNPs with  
 105 minor allele frequency (estimated using 1000 Genomes Project<sup>4</sup> data) greater than 5% in  
 106 both populations, which is a set of SNPs that are well imputed in diverse populations and  
 107 has been used in previous studies.<sup>3,7</sup>

108 We use weighted least square regression to obtain estimates of  $\tau_{1C}$ ,  $\tau_{2C}$ , and  $\theta_C$ . For  
 109 estimating  $\tau_{pC}$ , we use weights similar to those described in Finucane et al 2015. In detail,

110 the weights for each regression SNP  $j$  in population  $p$  is

$$w_{pj} = \frac{1}{\ell_p(j, \text{HapMap3}) (N_p \sum_C \ell_p(j, C) \tau_{pC} + 1)^2}. \quad (20)$$

111 For estimating  $\theta_C$ , we use the following weights

$$v_{pj} = \frac{1}{\sqrt{\prod_{p=1}^2 \ell_p(j, \text{HapMap3}) \left[ \prod_{p=1}^2 (N_p \sum_C \ell_p(j, C) \tau_{pC} + 1) + N_p \sum_C \ell_x(j, C) \theta_C \right]}}. \quad (21)$$

## 112 Estimating stratified squared trans-ethnic genetic correlation

113 Let  $\hat{\tau}_{1C}$ ,  $\hat{\tau}_{2C}$ , and  $\hat{\theta}_C$ , be the estimates of  $\tau_{1C}$ ,  $\tau_{2C}$ , and  $\theta_C$ , respectively. First, we obtain  
 114 estimates of stratified trans-ethnic genetic covariance and heritability of a binary annotation  
 115  $C$  as,

$$\begin{aligned} \hat{\rho}_g(C) &= \sum_{j \in C} \sum_{C'} a_{C'}(j) \hat{\theta}_{C'}, \\ \hat{h}_{g1}^2(C) &= \sum_{j \in C} \sum_{C'} a_{C'}(j) \hat{\tau}_{1C'}, \\ \hat{h}_{g2}^2(C) &= \sum_{j \in C} \sum_{C'} a_{C'}(j) \hat{\tau}_{2C'}. \end{aligned} \quad (22)$$

116 We jackknife over 200 continuous and disjoint blocks of SNPs to obtain standard error of  
 117 each estimates. As, an example, we estimate standard error of  $\hat{\rho}_g(C)$  as

$$\text{S.E.}[\hat{\rho}_g(C)] = \sqrt{\frac{B-1}{B} \sum_{b=1}^B \left[ \hat{\rho}_g(C) - \hat{\rho}_g^{(b)}(C) \right]^2}, \quad (23)$$

118 where  $B$  is the total number of jackknife samples, and  $\hat{\rho}_g^{(b)}(C)$  denotes the estimate with  
 119 SNPs in the  $b$ -th block removed.

120 Next, we obtain an initial estimate of stratified squared trans-ethnic genetic correlation,  
 121  $r_g^2(C)$ , as

$$\tilde{r}_g^2(C) = \frac{\hat{\rho}_g^2(C) - (\text{S.E.}[\hat{\rho}_g(C)])^2}{\hat{h}_{g1}^2(C) \hat{h}_{g2}^2(C) - \text{Cov}[\hat{h}_{g1}^2(C), \hat{h}_{g2}^2(C)]}, \quad (24)$$

122 where  $\text{Cov}[\hat{h}_{g1}^2(C), \hat{h}_{g2}^2(C)]$  is estimated using jackknife over 200 continuous and disjoint



123 blocks of SNPs,

$$\text{Cov}[\hat{h}_{g1}^2(C), \hat{h}_{g2}^2(C)] = \frac{B-1}{B} \sum_{b=1}^B [\hat{h}_{g1}^2(C) - \hat{h}_{g1}^{2(b)}(C)] [\hat{h}_{g2}^2(C) - \hat{h}_{g2}^{2(b)}(C)]. \quad (25)$$

124 The initial estimator,  $\tilde{r}_g^2(C)$ , however, is a biased estimator of  $r_g^2(C)$ .<sup>9</sup> We estimate and  
 125 correct for the bias using jackknife samples of  $\tilde{r}_g^2(C)$ .<sup>9</sup> We obtain final bias-corrected estimate  
 126 of  $r_g^2(C)$  as,

$$\hat{r}_g^2(C) = \left\{ \tilde{r}_g^2(C) + \frac{\text{Cov}[\hat{\rho}_g^2(C), \hat{h}_{g1}^2(C)\hat{h}_{g2}^2(C)]}{\hat{h}_{g1}^2(C)\hat{h}_{g2}^2(C)} \right\} / \left\{ 1 + \frac{\text{Var}[\hat{h}_{g1}^2(C)\hat{h}_{g2}^2(C)]}{\hat{h}_{g1}^2(C)\hat{h}_{g2}^2(C)} \right\}, \quad (26)$$

127 and obtain its standard error using block jackknife.

128 We obtain an initial estimate enrichment of stratified squared trans-ethnic genetic cor-  
 129 relation

$$\tilde{\lambda}^2(C) = \frac{\hat{r}_g^2(C)}{\hat{r}_g^2}, \quad (27)$$

130 and obtain bias corrected enrichment as

$$\hat{\lambda}^2(C) = \left\{ \tilde{\lambda}^2(C) + \frac{\text{Cov}[\hat{r}_g^2(C), \hat{r}_g^2]}{\hat{r}_g^2(C)} \right\} / \left\{ 1 + \frac{\text{Var}[\hat{r}_g^2(C)]}{\hat{r}_g^2(C)} \right\} \quad (28)$$

131

## 132 Shrinkage estimator

133 Estimates of  $r_g^2(C)$  can be imprecise and unreliable if the denominator,  $h_{g1}^2(C)h_{g2}^2(C)$ ,  
 134 is noisy and close to 0. This is especially true for small annotations. To mitigate this issue,  
 135 we introduce a shrinkage estimator to “regularize” the estimates of  $r_g^2(C)$ .

136 We apply the shrinkage to estimates of stratified per-SNP genetic covariance and heri-  
 137 tability, so that the per-SNP estimates are shrunk towards genome-wide average. Inspired  
 138 by Bayesian shrinkage, we derive a shrinkage factor for per-SNP genetic covariance and

139 heritability as follows. Let

$$\begin{aligned}
\gamma_1 &= 1 / \left( 1 + \alpha \frac{\text{Var} [\hat{\rho}_g(C)]}{\text{Var} [\hat{\rho}_g]} \frac{M}{M_C} \right), \\
\gamma_2 &= 1 / \left( 1 + \alpha \frac{\text{Var} [\hat{h}_{g1}(C)]}{\text{Var} [\hat{h}_{g1}^2]} \frac{M}{M_C} \right), \\
\gamma_3 &= 1 / \left( 1 + \alpha \frac{\text{Var} [\hat{h}_{g2}(C)]}{\text{Var} [\hat{h}_{g2}^2]} \frac{M}{M_C} \right),
\end{aligned} \tag{29}$$

140 where  $M_C$  is the number of SNPs in annotation  $C$ , and  $\alpha \in [0, 1]$  is a user-controlled tuning  
141 parameter that governs the magnitude of shrinkage. We define the shared shrinkage factor  
142 as

$$\gamma = \min\{\gamma_1, \gamma_2, \gamma_3\}. \tag{30}$$

143 We use shared shrinkage factor instead of separate shrinkage factors for convenience of char-  
144 acterizing the behavior of the estimator. When  $\alpha$  is set to 0, no shrinkage is applied; when  
145  $\alpha$  is set to 1, the entire Bayesian shrinkage is applied.

146 We apply the shrinkage to stratified genetic covariance and heritability as follows,

$$\begin{aligned}
\bar{\rho}_g(C) &= M_C \left( \gamma \frac{\hat{\rho}_g(C)}{M_C} + (1 - \gamma) \frac{\hat{\rho}_g}{M} \right) \\
\bar{h}_{g1}^2(C) &= M_C \left( \gamma \frac{\hat{h}_{g1}^2(C)}{M_C} + (1 - \gamma) \frac{\hat{h}_{g1}^2}{M} \right) \\
\bar{h}_{g2}^2(C) &= M_C \left( \gamma \frac{\hat{h}_{g2}^2(C)}{M_C} + (1 - \gamma) \frac{\hat{h}_{g2}^2}{M} \right),
\end{aligned} \tag{31}$$

147 and obtain standard errors of the shrunk estimates using block jackknife. Intuitively, if  
148 stratified heritability and trans-ethnic genetic covariance are estimated with low variance,  
149 the amount of shrinkage needed will be small, and shrinkage estimator will preserve the  
150 unshrunk estimates. On the other hand, if stratified heritability and genetic covariance are  
151 estimated with large variance (i.e. noisy), the shrinkage estimator will shrink the estimates  
152 towards genome-wide average.

153 Finally, we obtain shrunk  $r_g^2(C)$  and  $\lambda^2(C)$ ,  $\bar{r}_g^2(C)$  and  $\bar{\lambda}^2(C)$ , by plugging in  $\bar{\rho}_g(C)$ ,  
154  $\bar{h}_{g1}^2(C)$ , and  $\bar{h}_{g2}^2(C)$  into the procedures described in previous section. We found that when  
155  $\alpha = 0.5$ , the shrinkage estimator yields robust results across a wide range of polygenicity.

156 **Two-population Eyre-Walker model**

157 The Eyre-Walker model<sup>10</sup> couples fitness effect (selection coefficient) with causal disease  
 158 effect size,  $\beta$ , through the equation

$$\beta = \delta S^\tau (1 + \epsilon), \quad (32)$$

159 where  $\delta = \pm 1$  with equal probabilities governs the sign of  $\beta$ ;  $S = 4sN_e$  ( $s$  is the fitness effect,  
 160  $N_e$  effective sample size of the population);  $\tau$  is the parameter coupling selection and  $\beta$ ; and  
 161  $\epsilon$  is normally distributed with mean 0 and variance  $\sigma_\epsilon^2$ . Since the scaling factor  $4N_e$  does  
 162 not affect trans-ethnic genetic correlation (and subsequently enrichment of stratified squared  
 163 trans-ethnic genetic correlation,  $\lambda^2(C)$ ), we use the simplified equation instead,

$$\beta \propto \delta s^\tau (1 + \epsilon). \quad (33)$$

164 We use negative  $s$  to denote deleteriousness, following convention of previous works.<sup>11,12</sup>  
 165 However, we emphasize that positive  $s$  (i.e. beneficial mutations) is also plausible.

166 We extend the Eyre-Walker model to two populations to model causal disease effect  
 167 sizes of SNP  $j$ ,  $\beta_{1j}$  and  $\beta_{2j}$ , in population 1 and population 2, respectively,

$$\begin{aligned} \beta_{1j} &\propto \delta s_{1j}^\tau (1 + \epsilon_1), \\ \beta_{2j} &\propto \delta s_{2j}^\tau (1 + \epsilon_2), \end{aligned} \quad (34)$$

168 where  $s_{1j}$  and  $s_{2j}$  are the fitness effects of SNP  $j$  in the two populations;  $\epsilon_1$  and  $\epsilon_2$  indepen-  
 169 dently follow normal distributions with mean 0 and variance  $\sigma_1^2$  and  $\sigma_2^2$ . Assuming  $\tau$  is a  
 170 constant,  $\beta_{1j}$  and  $\beta_{2j}$  has covariance,

$$\text{Cov}[\beta_{1j}, \beta_{2j}] \propto E[\delta s_{1j}^\tau (1 + \epsilon_1) \delta s_{2j}^\tau (1 + \epsilon_2)] = E[(s_{1j} s_{2j})^\tau], \quad (35)$$

171 and variance,

$$\begin{aligned} \text{Var}[\beta_{1j}] &\propto E[(\delta s_{1j}^\tau (1 + \epsilon_1))^2] = E[s_{1j}^{2\tau} (1 + \sigma_1^2)], \\ \text{Var}[\beta_{2j}] &\propto E[(\delta s_{2j}^\tau (1 + \epsilon_2))^2] = E[s_{2j}^{2\tau} (1 + \sigma_2^2)]. \end{aligned} \quad (36)$$

172

The squared genome-wide trans-ethnic genetic correlation is then

$$\begin{aligned} r_g^2 &= \frac{(\sum_j \mathbb{E}[(s_{1j}s_{2j})^\tau])^2}{(\sum_j \mathbb{E}[s_{1j}^{2\tau}](1 + \sigma_e^2) \mathbb{E}[s_{2j}^{2\tau}](1 + \sigma_e^2))} \\ &= \frac{1}{(1 + \sigma_1^2)(1 + \sigma_2^2)} \frac{(\sum_j \mathbb{E}[(s_{1j}s_{2j})^\tau])^2}{\sum_j \mathbb{E}[s_{1j}^{2\tau}] \mathbb{E}[s_{2j}^{2\tau}]} . \end{aligned} \quad (37)$$

173

And the stratified squared trans-ethnic genetic correlation of a binary annotation  $C$  is

$$\begin{aligned} r_g^2(C) &= \frac{(\sum_{j \in C} \mathbb{E}[(s_{1j}s_{2j})^\tau])^2}{(\sum_{j \in C} \mathbb{E}[s_{1j}^{2\tau}](1 + \sigma_e^2) \mathbb{E}[s_{2j}^{2\tau}](1 + \sigma_e^2))} \\ &= \frac{1}{(1 + \sigma_1^2)(1 + \sigma_2^2)} \frac{(\sum_{j \in C} \mathbb{E}[(s_{1j}s_{2j})^\tau])^2}{\sum_{j \in C} \mathbb{E}[s_{1j}^{2\tau}] \mathbb{E}[s_{2j}^{2\tau}]} . \end{aligned} \quad (38)$$

174

The enrichment of squared trans-ethnic genetic correlation,  $\lambda^2(C)$ , only depends on  $s_{1j}$  and

175

$s_{2j}$ ,

$$\lambda^2(C) = \frac{r_g^2(C)}{r_g^2} = \frac{(\sum_{j \in C} \mathbb{E}[(s_{1j}s_{2j})^\tau])^2}{(\sum_{j \in C} \mathbb{E}[s_{1j}^{2\tau}] \mathbb{E}[s_{2j}^{2\tau}])} \frac{(\sum_j \mathbb{E}[s_{1j}^{2\tau}] \mathbb{E}[s_{2j}^{2\tau}])}{(\sum_j \mathbb{E}[(s_{1j}s_{2j})^\tau])^2} . \quad (39)$$

176

Therefore, although  $r_g^2$  can be less than 1 as long as  $\sigma_1^2$  or  $\sigma_2^2$  is greater than 0, differential

177

fitness effects in annotation  $C$  compared with genome-wide average is necessary for  $\lambda^2(C)$

178

to be different from 1.

179

To introduce population-specific fitness effects, we assume

$$\begin{aligned} s_1 &= s_0(1 + \Delta_1), \\ s_2 &= s_0(1 + \Delta_2), \end{aligned} \quad (40)$$

180

where  $s_0$  represents the fitness effect prior to the split of population 1 and population 2, and

181

$\Delta_1$  and  $\Delta_2$  represent the relative change in fitness effects since the split, and are indepen-

182

dently sampled from  $N(0, \sigma_\Delta^2)$  (and truncated so that  $(1 + \Delta_1)$  and  $(1 + \Delta_2)$  are non-negative).

183

We further assume that  $\sigma_\Delta^2$  is small (close to zero) at weakly deleterious or effectively neutral

184

SNPs (i.e.  $s_1 \approx s_2$ ), and large at more strongly deleterious SNPs (i.e.  $s_1 \neq s_2$ ) (Supple-

185

mentary Figure 31a). Under our model, fitness effects in the two populations have the same

186

mean, but higher variance at SNPs with large fitness effect (i.e. strongly deleterious SNPs)

187

and lower variance at SNPs with small fitness effect (i.e. weakly deleterious SNPs). Since

188

both populations have the same mean fitness effect, we expect the relationship between effect

189

size and MAF to be the same in the two populations for strongly and weakly deleterious

190

SNPs. We have publicly released Python code implementing the 2-population Eyre-Walker

191

model (see Code availability).

192 We used Equation (40) to sample population-specific fitness effects ( $s_1$  and  $s_2$ ) and  
 193 subsequently used Equation (34) to sample causal disease effect sizes ( $\beta_1$  and  $\beta_2$ ) for 50,000  
 194 simulated unlinked SNPs, setting 90% of the SNPs to be weakly deleterious ( $s_0 = -10^{-5}$ )  
 195 and 10% of the SNPs to be more strongly deleterious ( $s_0 = -10^{-4}$ ) (Methods). We then  
 196 used the sampled causal effect sizes to compute the enrichment/depletion of squared trans-  
 197 ethnic genetic correlation ( $\lambda^2(C)$ ) for SNPs in each of these two categories. When  $\tau = 0.2$ ,  
 198  $\sigma_1^2 = \sigma_2^2 = 1.0$ , and  $\sigma_\Delta^2 = 0.0$  for both weakly and more strongly deleterious SNPs (i.e. same  
 199 fitness effects across populations),  $\lambda^2(C)$  was equal to 1.00 (s.e. 0.00) for both categories  
 200 (Supplementary Figure 31b). However, when  $\sigma_\Delta^2 = 0.0$  for weakly deleterious SNPs but  
 201  $\sigma_\Delta^2 = 0.7$  for more strongly deleterious SNPs (leaving all other parameters unchanged),  
 202  $\lambda^2(C)$  for more strongly deleterious SNPs decreased to 0.79 (s.e. 0.01) (Supplementary  
 203 Figure 31c) due to more population-specific causal disease effect sizes, roughly matching  
 204 results for SNPs in the top quintile of background selection statistic in real data analyses  
 205 (Figure 2). Analyses at other values of  $\tau$  produced similar results, yielding lower values of  
 206  $\lambda^2(C)$  for more strongly deleterious SNPs at higher values of  $\sigma_\Delta^2$  (Supplementary Table 6).  
 207 We also performed a secondary analysis with  $\sigma_\Delta^2 = 0.7$  for both weakly and more strongly  
 208 deleterious SNPs (leaving all other parameters unchanged). We observed no depletion of  
 209  $\lambda^2(C)$  at more strongly deleterious SNPs (Supplementary Figure 32). Thus, we concluded  
 210 that, under the Eyre-Walker evolutionary model, a lower  $\sigma_\Delta^2$  at weakly deleterious SNPs and  
 211 a higher  $\sigma_\Delta^2$  at more strongly deleterious SNPs is necessary to explain the results observed  
 212 in analyses of real traits.

213 Here, we did not consider demographic histories in our evolutionary modeling, which  
 214 may lead to increased proportions of population-specific variants, decreasing trans-ethnic  
 215 polygenic risk score accuracy.<sup>13</sup> We also note that other evolutionary models<sup>14,15</sup> exist, and  
 216 could also be explored.<sup>14,15</sup>

217 **Supplementary tables**

simulated $r_g$	estimated $r_g$	s.e. mean	mean jackknife s.e.
0	0	0.0016	0.0016
0.2	0.21	0.0015	0.0016
0.4	0.41	0.0016	0.0017
0.6	0.62	0.0017	0.0017
0.8	0.82	0.0018	0.0019
1	1.03	0.002	0.0021

Supplementary Table 1: **Numerical results of S-LDXR in estimating genome-wide trans-ethnic genetic correlation.** Mean and standard errors are based on 1,000 simulations.

trait (abbrev.)	$N_{EAS}$	$N_{EUR}$	$h_{g,EAS}^2$	$h_{g,EUR}^2$	$r_g$
*Atrial Fibrillation (AF)	36792 <sup>16</sup>	1030836 <sup>17</sup>	0.110 (0.026)	0.021 (0.002)	0.817 (0.193)
Age at Menarche (AMN)	67029 <sup>18</sup>	252514 <sup>19</sup>	0.074 (0.013)	0.128 (0.010)	0.878 (0.057)
Age at Menopause (AMP)	43861 <sup>18</sup>	69360 <sup>19</sup>	0.092 (0.021)	0.190 (0.016)	0.567 (0.091)
Basophil Count (BASO)	62076 <sup>20</sup>	131860 <sup>21</sup>	0.107 (0.018)	0.088 (0.011)	0.427 (0.061)
Body Mass Index (BMI)	158284 <sup>20</sup>	337539 <sup>22</sup>	0.161 (0.010)	0.207 (0.007)	0.804 (0.021)
Blood Sugar (BS)	93146 <sup>20</sup>	337539 <sup>22</sup>	0.057 (0.011)	0.036 (0.004)	0.829 (0.087)
Diastolic Blood Pressure (DBP)	136615 <sup>20</sup>	337539 <sup>22</sup>	0.052 (0.008)	0.146 (0.007)	0.862 (0.059)
Estimated Glomerular Filtration Rate (EGFR)	143658 <sup>20</sup>	100125 <sup>23</sup>	0.074 (0.008)	0.058 (0.007)	1.053 (0.063)
Eosinophil Count (EO)	62076 <sup>20</sup>	337539 <sup>22</sup>	0.076 (0.016)	0.154 (0.010)	0.950 (0.092)
Hemoglobin A1c (HBA1C)	42790 <sup>20</sup>	337539 <sup>22</sup>	0.109 (0.022)	0.082 (0.006)	0.875 (0.083)
High Density Lipoprotein (HDL)	70657 <sup>20</sup>	337539 <sup>22</sup>	0.109 (0.016)	0.140 (0.010)	0.892 (0.056)
Height (HEIGHT)	151569 <sup>24</sup>	337539 <sup>22</sup>	0.371 (0.017)	0.366 (0.018)	0.897 (0.018)
Hemoglobin (HGB)	108769 <sup>20</sup>	132596 <sup>21</sup>	0.070 (0.010)	0.166 (0.012)	0.911 (0.058)
Hematocrit (HTC)	108757 <sup>20</sup>	132699 <sup>21</sup>	0.078 (0.009)	0.161 (0.012)	0.870 (0.054)
Low Density Lipoprotein (LDL)	72866 <sup>20</sup>	337539 <sup>22</sup>	0.047 (0.015)	0.076 (0.009)	0.662 (0.105)
Lymphocyte Count (LYMPH)	62076 <sup>20</sup>	337539 <sup>22</sup>	0.121 (0.015)	0.165 (0.011)	0.903 (0.059)
Mean Corpuscular Hemoglobin (MCH)	108054 <sup>20</sup>	337539 <sup>22</sup>	0.130 (0.014)	0.144 (0.010)	0.884 (0.049)
MCH Concentration (MCHC)	108728 <sup>20</sup>	132586 <sup>21</sup>	0.069 (0.010)	0.089 (0.010)	0.887 (0.077)
Mean Corpuscular Volume (MCV)	108256 <sup>20</sup>	132353 <sup>21</sup>	0.146 (0.015)	0.200 (0.015)	0.891 (0.048)
*Major Depressive Disorder (MDD)	10640 <sup>25</sup>	62984 <sup>26</sup>	0.354 (0.078)	0.202 (0.014)	0.342 (0.074)
Monocyte Count (MONO)	62076 <sup>20</sup>	337539 <sup>22</sup>	0.123 (0.015)	0.156 (0.012)	0.811 (0.048)
Neutrophil Count (NEUT)	62076 <sup>20</sup>	131564 <sup>21</sup>	0.123 (0.016)	0.163 (0.011)	0.766 (0.059)
Platelet Count (PLT)	108208 <sup>20</sup>	337539 <sup>22</sup>	0.157 (0.015)	0.214 (0.013)	0.879 (0.035)
*Rheumatoid Arthritis (RA)	22343 <sup>27</sup>	37598 <sup>27</sup>	0.219 (0.041)	0.191 (0.021)	0.872 (0.098)
Red Blood Cell Count (RBC)	108794 <sup>20</sup>	337539 <sup>22</sup>	0.105 (0.011)	0.167 (0.009)	0.924 (0.052)
Systolic Blood Pressure (SBP)	136597 <sup>20</sup>	337539 <sup>22</sup>	0.064 (0.008)	0.149 (0.007)	0.807 (0.043)
*Schizophrenia (SCZ)	13761 <sup>28</sup>	35737 <sup>28</sup>	0.908 (0.064)	0.868 (0.040)	0.945 (0.036)
*Type 2 Diabetes (T2D)	190559 <sup>29</sup>	141364 <sup>30</sup>	0.099 (0.007)	0.046 (0.006)	0.927 (0.048)
Total Cholesterol (TC)	128305 <sup>20</sup>	337539 <sup>22</sup>	0.057 (0.013)	0.087 (0.010)	0.910 (0.073)
Triglyceride (TG)	105597 <sup>20</sup>	337539 <sup>22</sup>	0.061 (0.010)	0.100 (0.009)	0.932 (0.066)
White Blood Cell Count (WBC)	107964 <sup>20</sup>	337539 <sup>22</sup>	0.103 (0.010)	0.156 (0.007)	0.848 (0.037)

Supplementary Table 2: **Details of 31 diseases and complex traits analyzed.** We report genome-wide heritability of the traits estimated using S-LDSC<sup>3,11</sup> conditioned on baseline-LD-v2.2 model annotations in each population, and trans-ethnic genetic correlation estimated using S-LDXR conditioned on baseline-LD-X model annotations. Heritability estimates for binary traits denote observed-scale heritability (\* denotes binary traits). Standard errors of the estimates are shown in parentheses. The prevalence of MDD is 2.2% and 7.3%<sup>31</sup> in UK Biobank<sup>32</sup> EAS (Chinese) and EUR population, respectively. The prevalence of schizophrenia (SCZ) is 0.33% and 0.52% in Asia and Europe, respectively.<sup>33</sup> The prevalence of type 2 diabetes (T2D) is 2.7% and 4.2%<sup>31</sup> in UK Biobank EAS (Chinese) and EUR populations.

decile	$h_{g,EAS}^2(C)$ enrch.	$h_{g,EUR}^2(C)$ enrch.	$\lambda^2(C)$ (s.e.)
1st	NA	NA	NA
2nd	NA	NA	NA
3rd	NA	NA	NA
4th	NA	NA	NA
5th	1.04 (0.15)	1.17 (0.08)	0.92 (0.09)
6th	1.02 (0.08)	1.05 (0.04)	0.91 (0.04)
7th	1.01 (0.05)	0.99 (0.03)	1.04 (0.03)
8th	1.04 (0.04)	1.07 (0.03)	0.97 (0.02)
9th	0.99 (0.04)	0.99 (0.02)	0.97 (0.02)
10th	0.91 (0.03)	0.90 (0.02)	0.95 (0.03)

Supplementary Table 3: **Enrichment of heritability and stratified squared trans-ethnic genetic correlation across 10 MAF bin annotations.** MAF bins containing no SNP with MAF > 5% in either East Asian (EAS) or European (EUR) populations are reported as “NA”. Standard errors are reported in parentheses.

quintile	$-1 \times$ distance to nearest exon			background selection statistic		
	$h_{g,EAS}^2(C)$ enrch.	$h_{g,EUR}^2(C)$ enrch.	$\lambda^2(C)$	$h_{g,EAS}^2(C)$ enrch.	$h_{g,EUR}^2(C)$ enrch.	$\lambda^2(C)$
1st	0.24 (0.030)	0.23 (0.023)	1.07 (0.050)	0.44 (0.026)	0.43 (0.020)	1.23 (0.052)
2nd	0.59 (0.019)	0.65 (0.013)	1.16 (0.028)	0.68 (0.014)	0.68 (0.011)	1.19 (0.025)
3rd	0.89 (0.020)	0.92 (0.014)	1.03 (0.022)	0.88 (0.010)	0.89 (0.0073)	1.06 (0.011)
4th	1.15 (0.028)	1.15 (0.019)	0.96 (0.021)	1.20 (0.012)	1.21 (0.0087)	0.91 (0.010)
5th	2.13 (0.062)	2.04 (0.042)	0.87 (0.018)	1.82 (0.037)	1.81 (0.027)	0.79 (0.016)

(a)

annotation	$\tau_{EAS}^*(C)$ (s.e.)	$\tau_{EUR}^*(C)$ (s.e.)	$\theta^*(C)$ (s.e.)
distance to nearest exon	0.020 (0.021)	-0.03 (0.018)	-0.015 (0.020)
background selection statistic	0.28 (0.027)	0.25 (0.020)	0.19 (0.021)

(b)

Supplementary Table 4: **Numerical S-LDXR results for distance to nearest exon annotation.** **a)** Heritability enrichment and enrichment of squared trans-ethnic genetic correlation ( $\lambda^2(C)$ ) of the reversed distance to nearest exon annotation and the background selection statistic annotation. Standard errors are displayed in parentheses. **b)** Standardized annotation effect sizes of the distance to nearest exon annotation and the background selection statistic annotation.



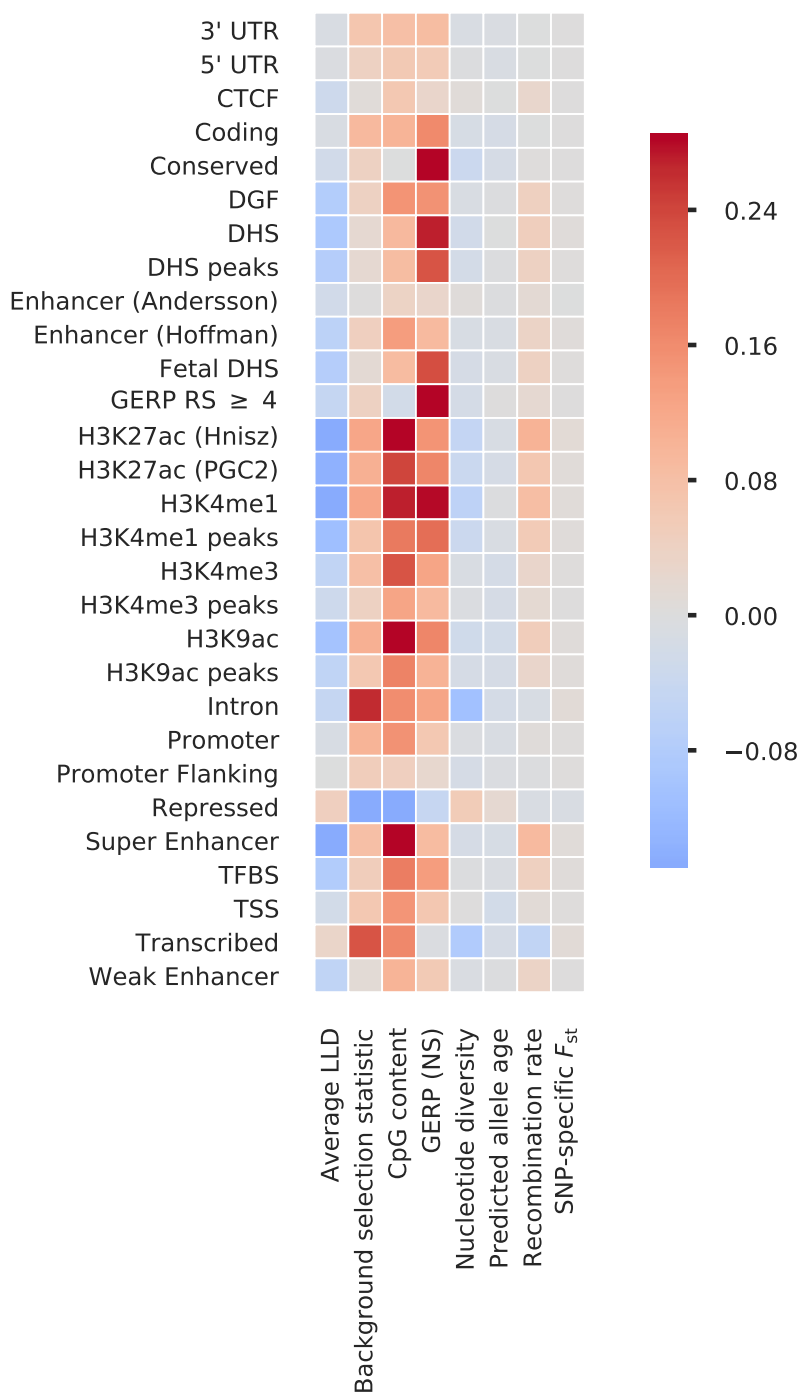
pLI decile	$h_{g,EAS}^2(C)$ enrch.	$h_{g,EUR}^2(C)$ enrch.	$\lambda^2(C)$
1st	1.39 (0.035)	1.38 (0.023)	0.851 (0.018)
2nd	1.62 (0.045)	1.56 (0.03)	0.863 (0.018)
3rd	1.68 (0.045)	1.57 (0.029)	0.9 (0.018)
4th	1.62 (0.045)	1.55 (0.03)	0.887 (0.019)
5th	1.68 (0.048)	1.65 (0.03)	0.871 (0.018)
6th	1.62 (0.047)	1.64 (0.031)	0.866 (0.019)
7th	1.55 (0.044)	1.55 (0.029)	0.922 (0.02)
8th	1.83 (0.044)	1.8 (0.03)	0.873 (0.018)
9th	1.95 (0.044)	1.92 (0.029)	0.888 (0.016)
10th	1.91 (0.04)	1.85 (0.023)	0.895 (0.015)

Supplementary Table 5: **Numerical S-LDXR results for deciles of probability of loss-of-function intolerance (pLI) annotations.**

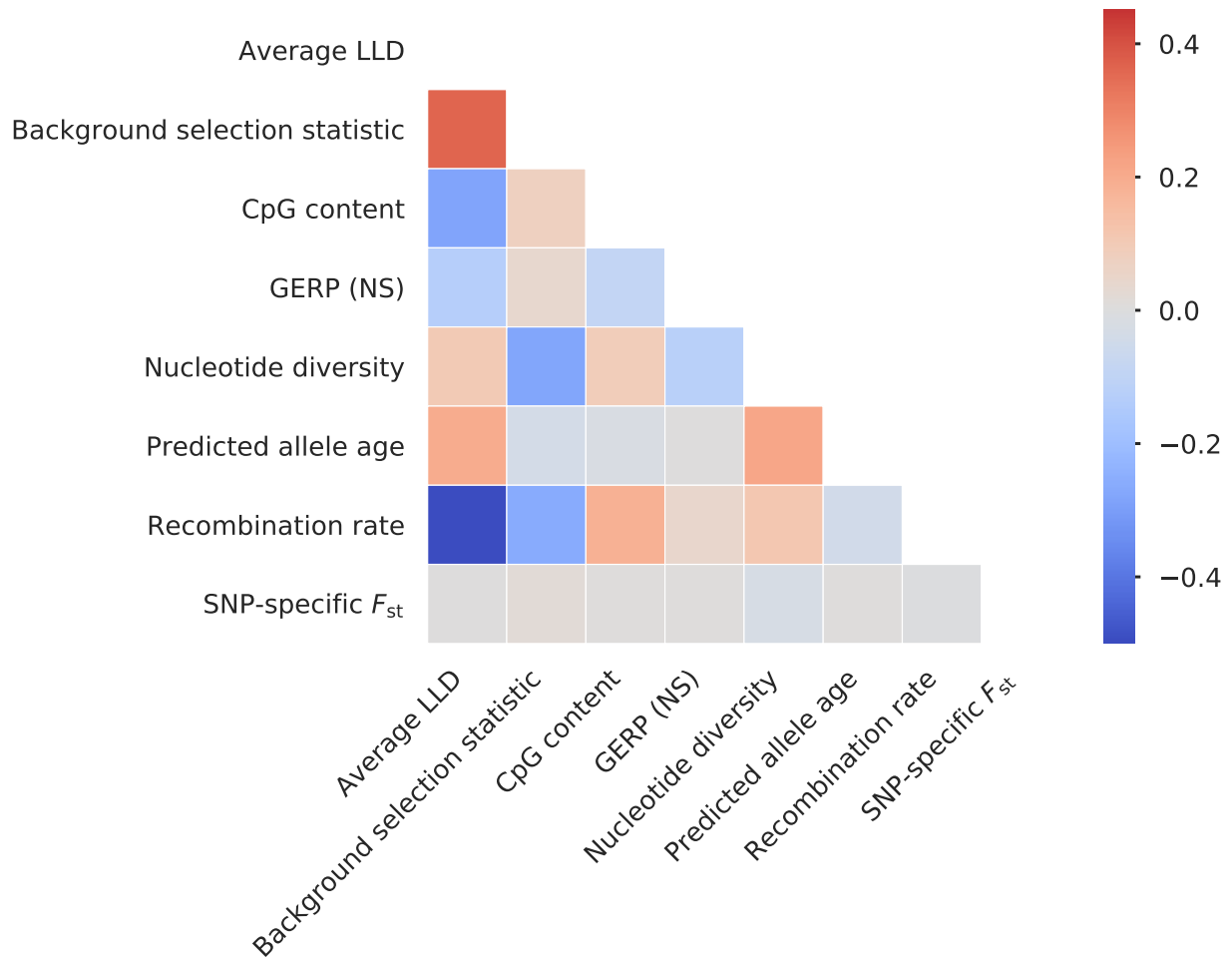
$\tau$	$\sigma_{\Delta}^2$	$h_{g1}^2(A)$ enrch.	$h_{g1}^2(B)$ enrch.	$h_{g2}^2(A)$ enrch.	$h_{g2}^2(B)$ enrch.	$\lambda^2(A)$	$\lambda^2(B)$
0	0	1.0 (0.002)	1.0 (0.02)	1.0 (0.002)	1.0 (0.02)	1.0 (0.0)	1.0 (0.0)
0	0.2	1.0 (0.002)	1.0 (0.02)	1.0 (0.002)	1.0 (0.02)	1.0 (0.0)	1.0 (0.0)
0	0.4	1.0 (0.002)	1.0 (0.02)	1.0 (0.002)	1.0 (0.02)	1.0 (0.0)	1.0 (0.0)
0	0.6	1.0 (0.002)	1.0 (0.02)	1.0 (0.002)	1.0 (0.02)	1.0 (0.0)	1.0 (0.0)
0	0.8	1.0 (0.002)	1.0 (0.02)	1.0 (0.002)	1.0 (0.02)	1.0 (0.0)	1.0 (0.0)
0	1	1.0 (0.002)	1.0 (0.02)	1.0 (0.002)	1.0 (0.02)	1.0 (0.0)	1.0 (0.0)
0.2	0	0.87 (0.004)	2.2 (0.03)	0.87 (0.004)	2.2 (0.03)	1.0 (0.0)	1.0 (0.0)
0.2	0.2	0.88 (0.004)	2.1 (0.03)	0.88 (0.004)	2.1 (0.03)	1.01 (0.0008)	0.96 (0.003)
0.2	0.4	0.89 (0.004)	2.1 (0.03)	0.89 (0.004)	2.1 (0.03)	1.03 (0.002)	0.88 (0.007)
0.2	0.6	0.89 (0.004)	2.01 (0.03)	0.89 (0.004)	2.01 (0.03)	1.05 (0.002)	0.82 (0.008)
0.2	0.8	0.89 (0.004)	2.0 (0.04)	0.89 (0.004)	2.0 (0.04)	1.06 (0.003)	0.76 (0.009)
0.2	1	0.89 (0.004)	2.0 (0.04)	0.89 (0.004)	2.0 (0.04)	1.07 (0.003)	0.72 (0.01)
0.4	0	0.65 (0.006)	4.12 (0.05)	0.65 (0.006)	4.12 (0.05)	1.0 (0.0)	1.0 (0.0)
0.4	0.2	0.66 (0.007)	4.08 (0.05)	0.66 (0.007)	4.08 (0.05)	1.04 (0.002)	0.94 (0.003)
0.4	0.4	0.66 (0.007)	4.07 (0.06)	0.66 (0.007)	4.07 (0.06)	1.10 (0.004)	0.87 (0.006)
0.4	0.6	0.66 (0.007)	4.07 (0.06)	0.66 (0.007)	4.07 (0.06)	1.14 (0.006)	0.81 (0.008)
0.4	0.8	0.66 (0.007)	4.09 (0.06)	0.66 (0.007)	4.09 (0.06)	1.18 (0.007)	0.76 (0.009)
0.4	1	0.65 (0.007)	4.11 (0.06)	0.65 (0.007)	4.11 (0.06)	1.21 (0.008)	0.73 (0.01)
0.6	0	0.40 (0.006)	6.38 (0.07)	0.40 (0.006)	6.38 (0.07)	1.0 (0.0)	1.0 (0.0)
0.6	0.2	0.40 (0.007)	6.44 (0.07)	0.40 (0.007)	6.44 (0.07)	1.12 (0.009)	0.94 (0.003)
0.6	0.4	0.39 (0.007)	6.52 (0.07)	0.39 (0.007)	6.52 (0.07)	1.24 (0.009)	0.88 (0.005)
0.6	0.6	0.38 (0.007)	6.61 (0.08)	0.38 (0.007)	6.61 (0.08)	1.35 (0.01)	0.84 (0.006)
0.6	0.8	0.37 (0.007)	6.70 (0.08)	0.37 (0.007)	6.70 (0.08)	1.44 (0.02)	0.81 (0.008)
0.6	1	0.36 (0.007)	6.77 (0.09)	0.36 (0.007)	6.77 (0.09)	1.52 (0.02)	0.79 (0.009)
0.8	0	0.21 (0.004)	8.16 (0.09)	0.21 (0.004)	8.16 (0.09)	1.0 (0.0)	1.0 (0.0)
0.8	0.2	0.19 (0.004)	8.30 (0.09)	0.19 (0.004)	8.30 (0.09)	1.23 (0.009)	0.95 (0.002)
0.8	0.4	0.18 (0.004)	8.42 (0.10)	0.18 (0.004)	8.42 (0.10)	1.47 (0.02)	0.92 (0.003)
0.8	0.6	0.16 (0.004)	8.52 (0.10)	0.16 (0.004)	8.52 (0.10)	1.67 (0.03)	0.90 (0.004)
0.8	0.8	0.15 (0.004)	8.61 (0.10)	0.15 (0.004)	8.61 (0.10)	1.84 (0.04)	0.89 (0.005)
0.8	1	0.15 (0.004)	8.69 (0.11)	0.15 (0.004)	8.69 (0.11)	1.99 (0.04)	0.88 (0.005)
1	0	0.092 (0.002)	9.18 (0.11)	0.092 (0.002)	9.18 (0.11)	1.0 (0.0)	1.0 (0.0)
1	0.2	0.078 (0.002)	9.30 (0.12)	0.078 (0.002)	9.30 (0.12)	1.39 (0.02)	0.97 (0.002)
1	0.4	0.067 (0.002)	9.39 (0.12)	0.067 (0.002)	9.39 (0.12)	1.75 (0.03)	0.96 (0.002)
1	0.6	0.060 (0.002)	9.46 (0.13)	0.060 (0.002)	9.46 (0.13)	2.06 (0.05)	0.95 (0.002)
1	0.8	0.054 (0.002)	9.51 (0.12)	0.054 (0.002)	9.51 (0.12)	2.32 (0.07)	0.95 (0.003)
1	1	0.050 (0.002)	9.55 (0.12)	0.050 (0.002)	9.55 (0.12)	2.54 (0.08)	0.95 (0.003)

Supplementary Table 6: **Numerical evolutionary modeling results using 2-population extension of Eyre-Walker model.** Standard errors of the mean are reported in parenthesis. Here,  $A$  refers to the set of SNPs with  $\bar{s} = -10^{-5}$ , and  $B$  the set of SNPs with  $\bar{s} = -10^{-4}$ . We use negative  $s$  to denote deleteriousness, following convention of previous works.<sup>11,12</sup> However, positive  $s$  (i.e. beneficial mutations) may also be plausible.

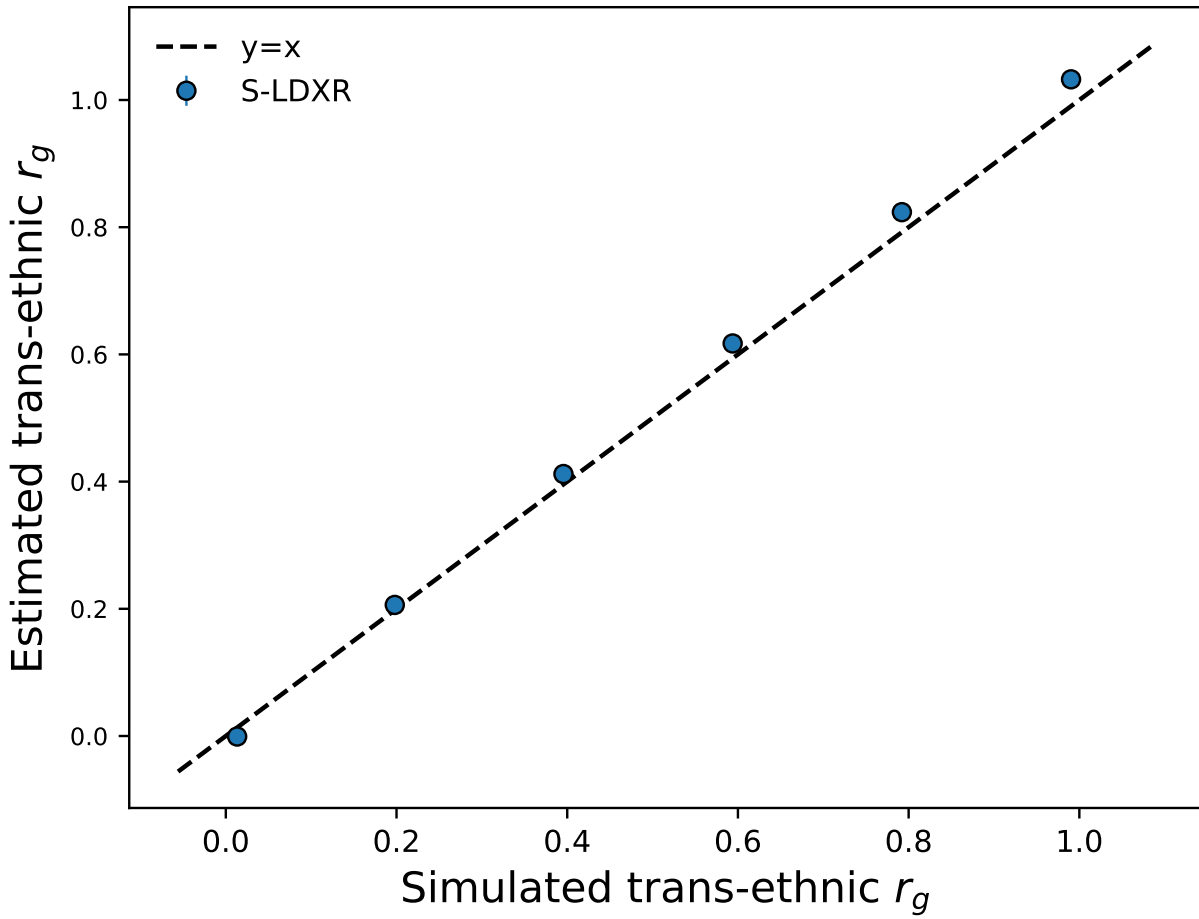
218 **Supplementary figures**



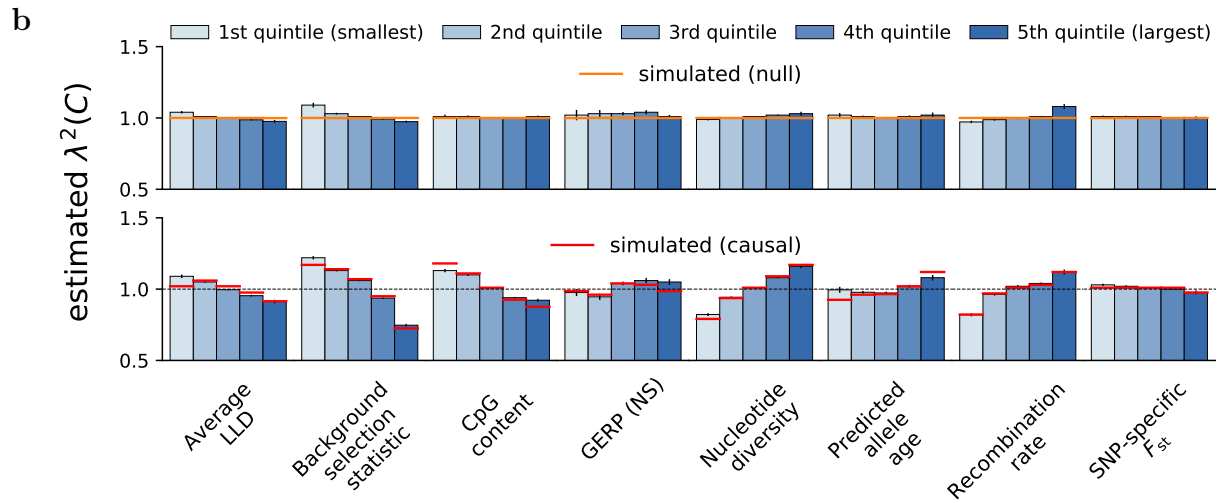
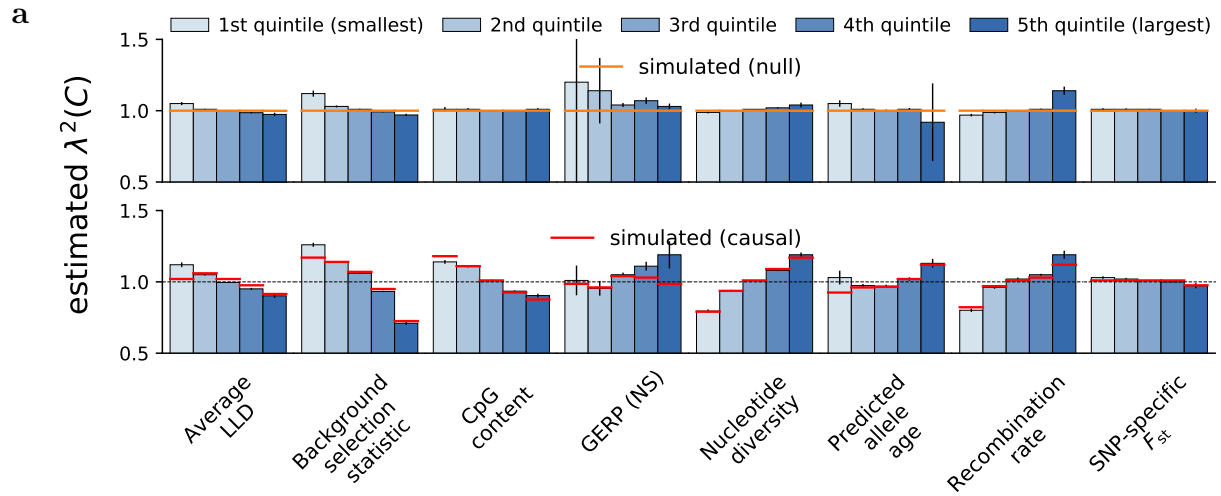
Supplementary Figure 1: **Correlation between functional annotations and continuous-valued annotations.** The correlations were computed across SNPs with minor allele frequency  $> 5\%$  in both populations.



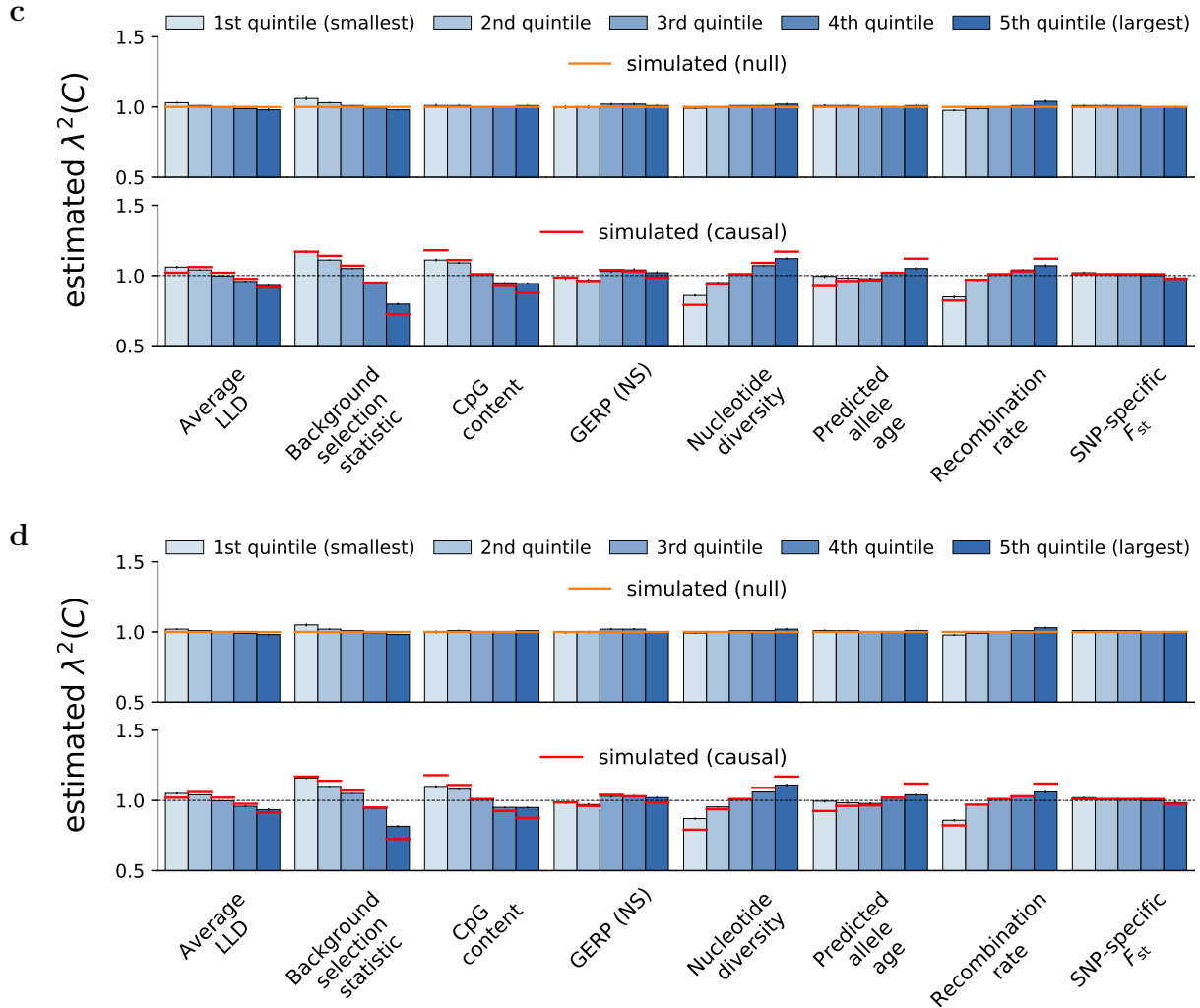
Supplementary Figure 2: **Correlation between continuous-valued annotations.** The correlations were computed across SNPs with minor allele frequency  $> 5\%$  in both populations.



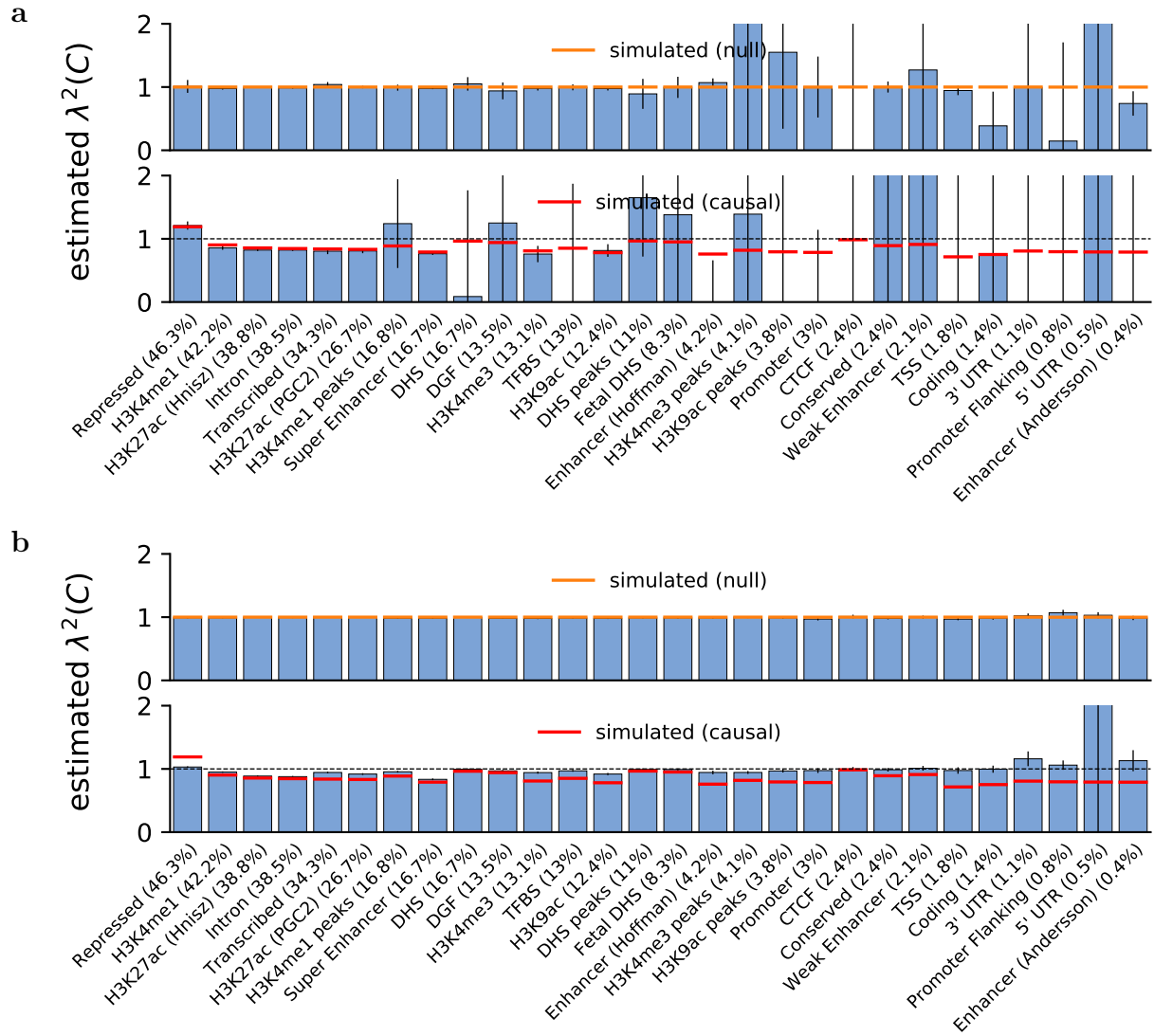
Supplementary Figure 3: **Accuracy of S-LDXR in estimating genome-wide trans-ethnic genetic correlation.** Here, 10% of SNPs are randomly selected to be causal. Mean and standard errors were obtained across 1,000 simulations. Error bars represent 1.96 times the standard error on both sides.



Supplementary Figure 4: (continued on next page)

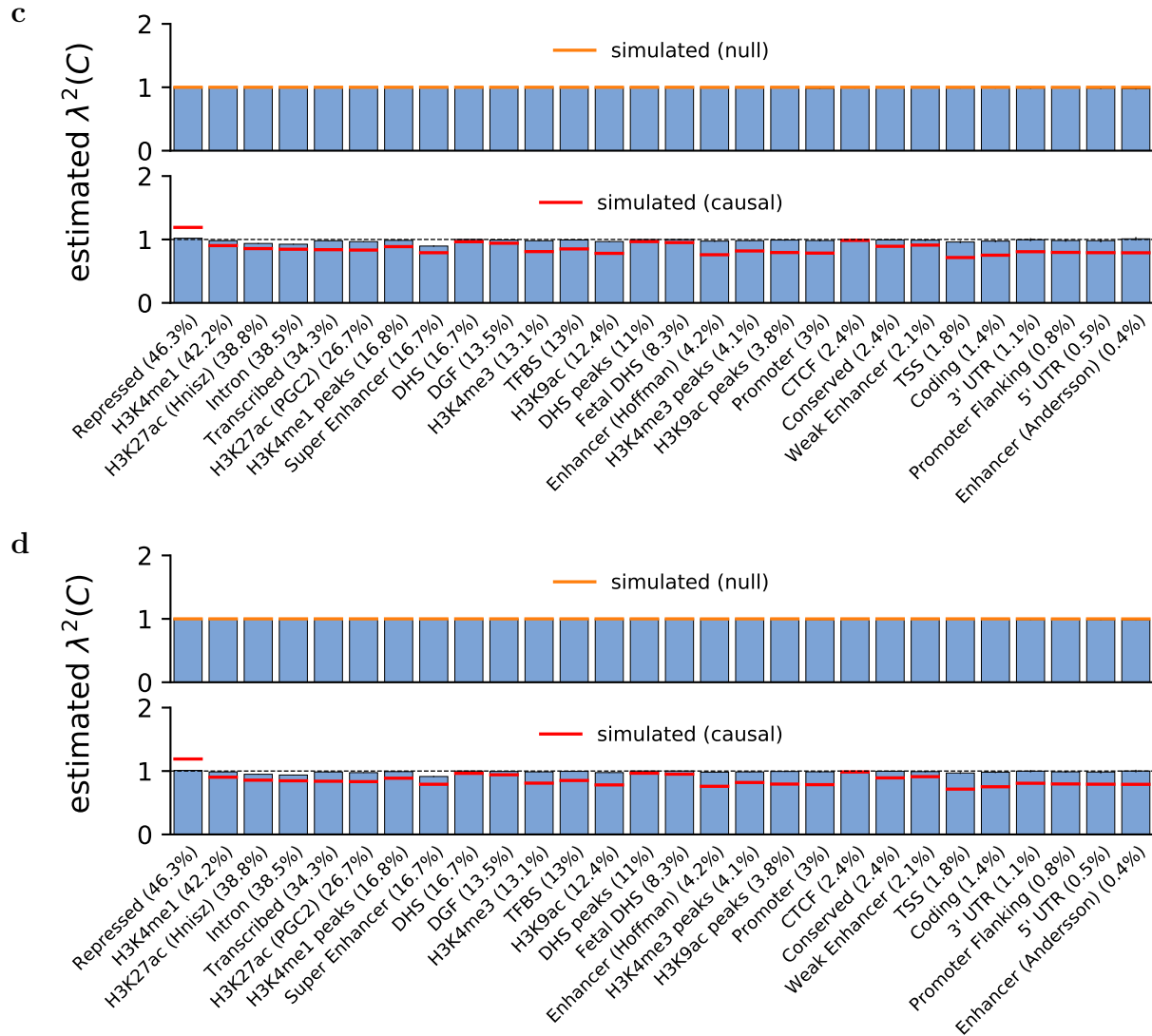


Supplementary Figure 4: **Accuracy of S-LDXR in estimating enrichment of stratified squared trans-ethnic genetic correlation,  $\lambda^2(C)$ , of quintiles of continuous-valued annotations.** Here, 10% of SNPs were randomly selected to be causal. Shrinkage level,  $\alpha$ , was set to 0.0 in **a**, 0.25 in **b**, 0.75 in **c**, and 1.0 in **d**. Mean and standard errors were obtained across 1,000 simulations. Error bars represent 1.96 times the standard error on both sides.



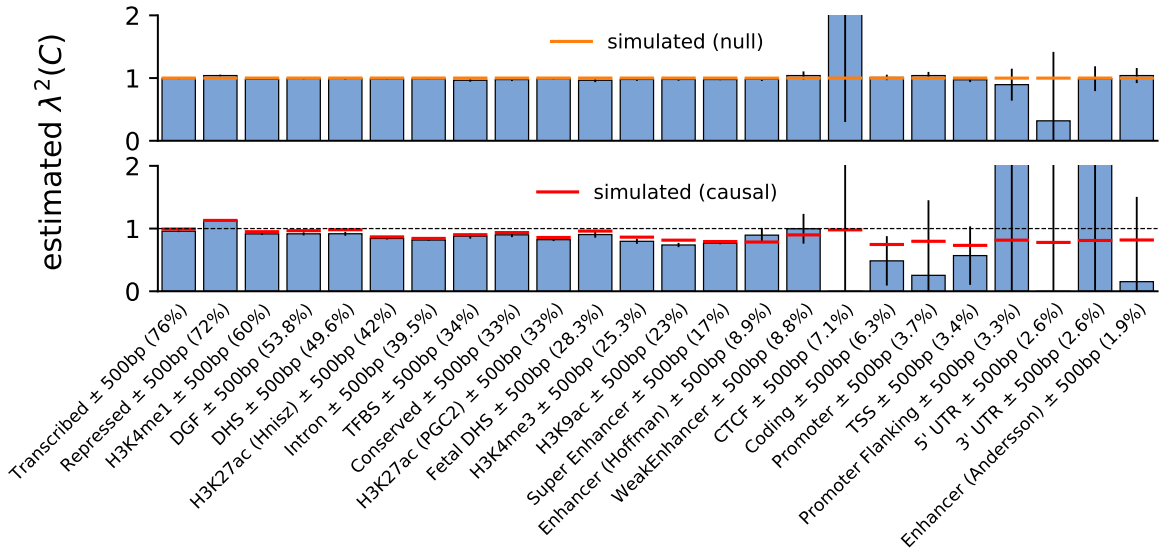
Supplementary Figure 5: (continued on next page)



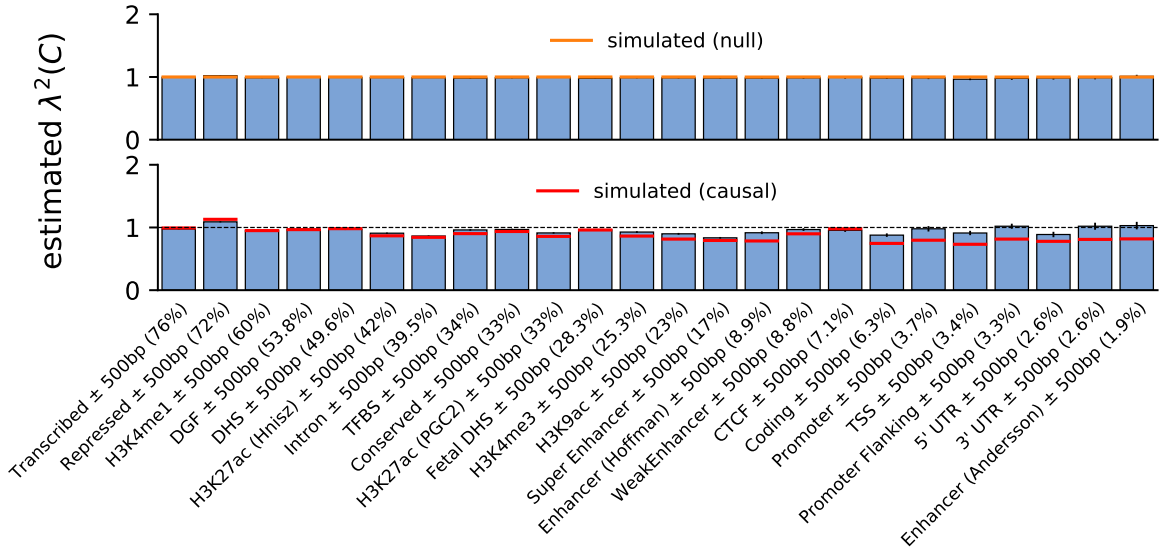


Supplementary Figure 5: **Accuracy of S-LDXR in estimating enrichment of stratified squared trans-ethnic genetic correlation,  $\lambda^2(C)$ , of functional annotations.** Here, 10% of SNPs were randomly selected to be causal. Shrinkage level,  $\alpha$ , was set to 0.0 in **a**, 0.25 in **b**, 0.75 in **c**, and 1.0 in **d**. Mean and standard errors were obtained across 1,000 simulations. Error bars represent 1.96 times the standard error on both sides.

a

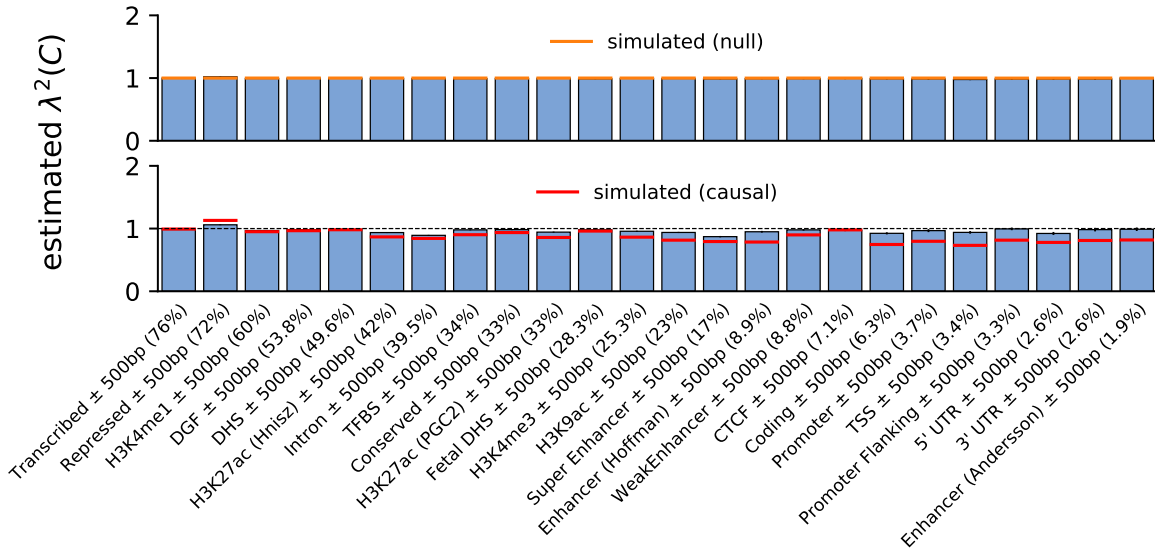


b

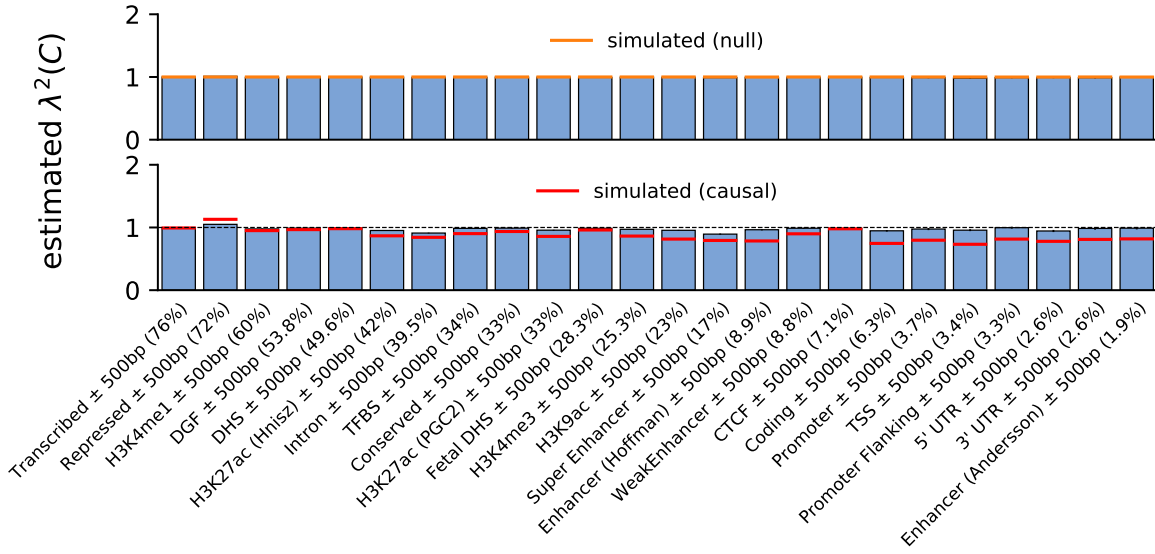


Supplementary Figure 6: (continued on next page)

c

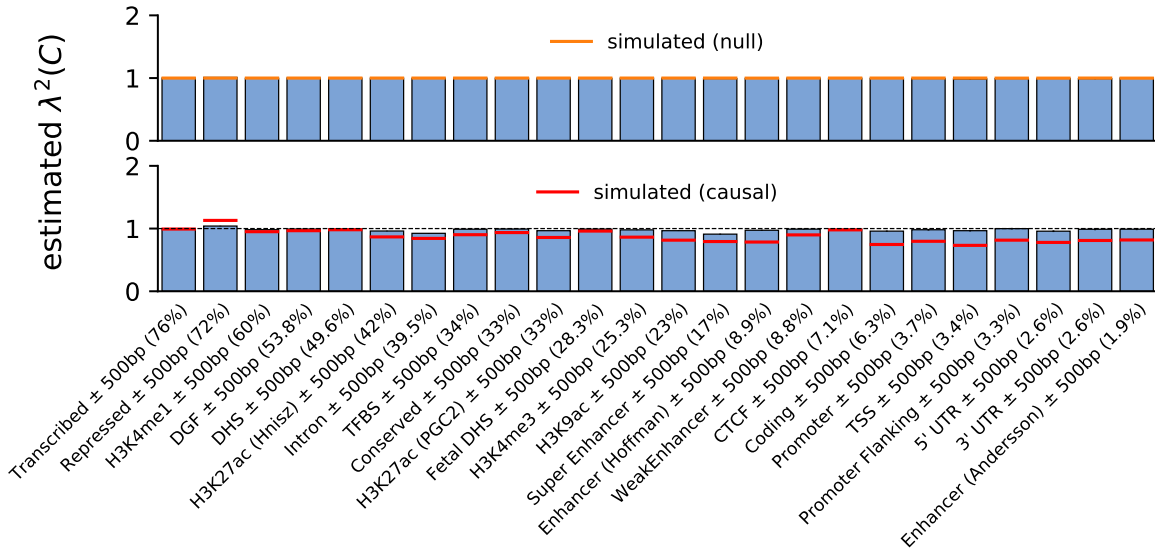


d

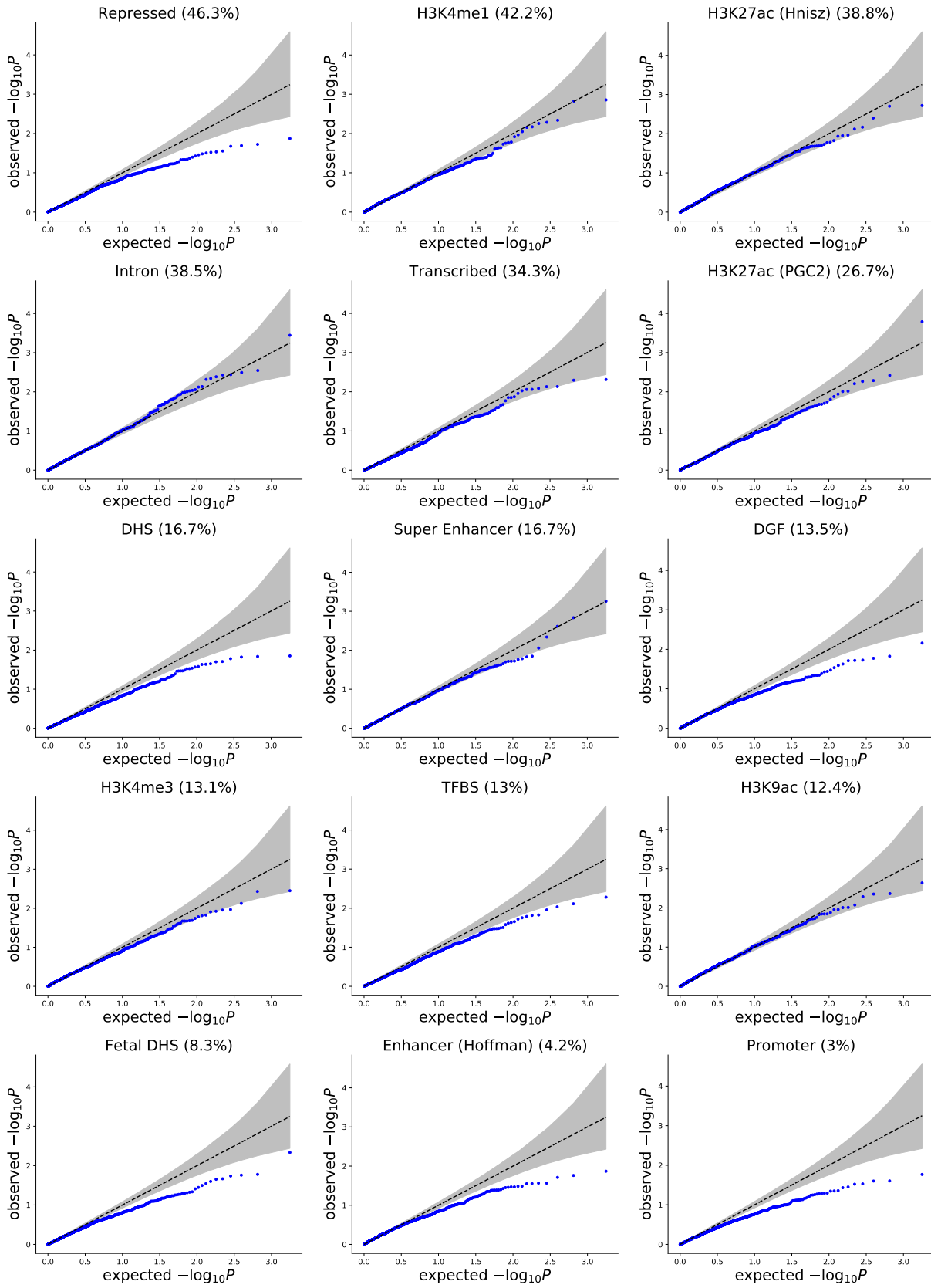


Supplementary Figure 6: (continued on next page)

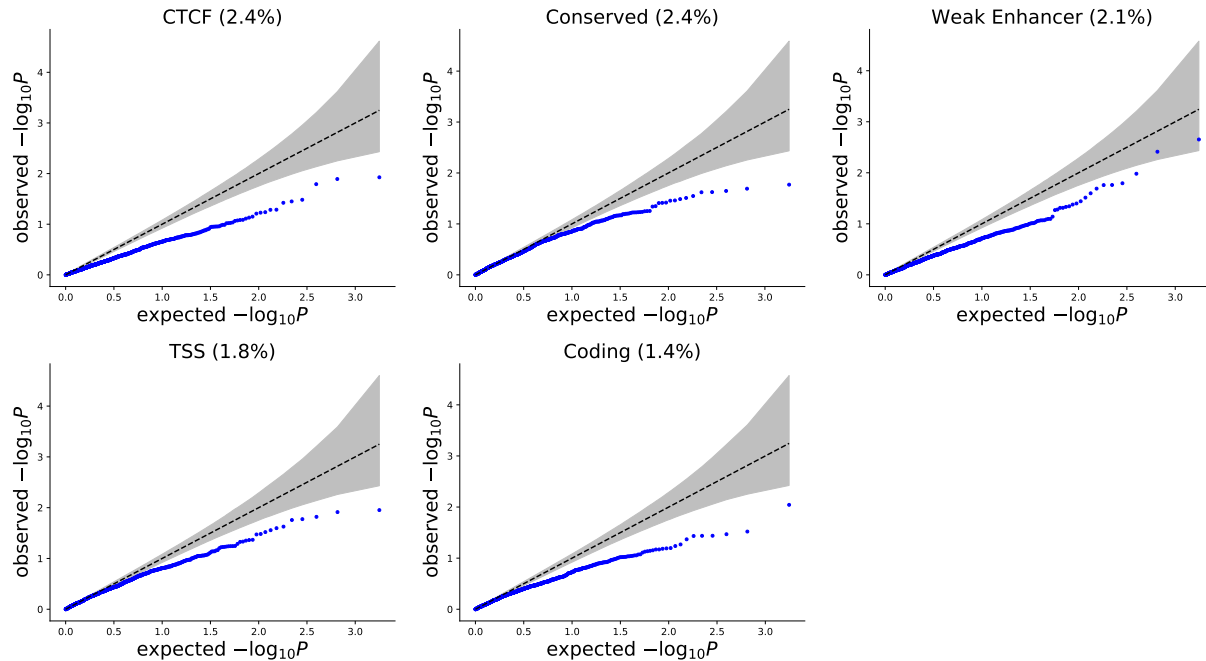
e



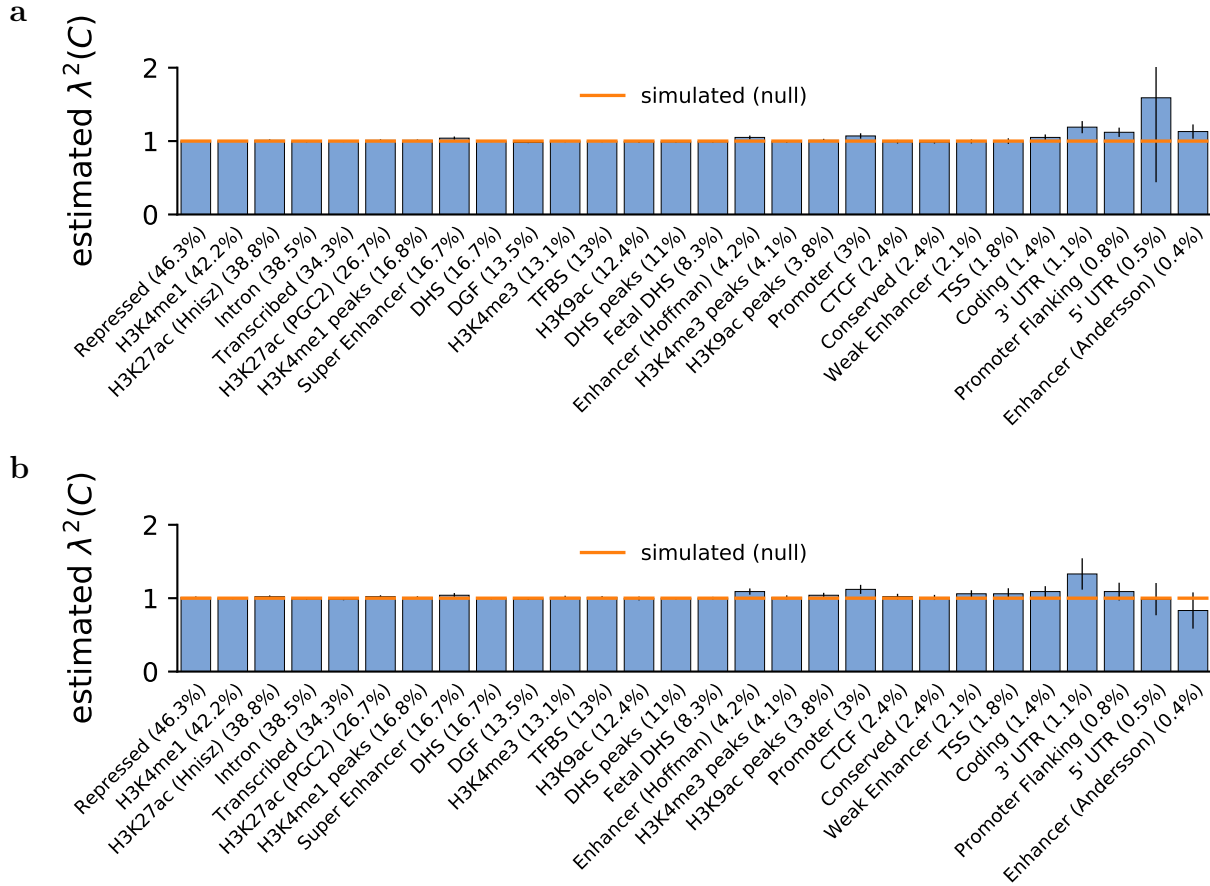
Supplementary Figure 6: **Accuracy of S-LDXR in estimating enrichment of stratified squared trans-ethnic genetic correlation,  $\lambda^2(C)$ , of 500-base-pair extended functional annotations.** Here, 10% of SNPs were randomly selected to be causal. Shrinkage level,  $\alpha$ , was set to 0.0 in **a**, 0.25 in **b**, 0.5 in **c**, 0.75 in **d**, and 1.0 in **e**. Mean and standard errors were obtained across 1,000 simulations. Error bars represent 1.96 times the standard error on both sides.



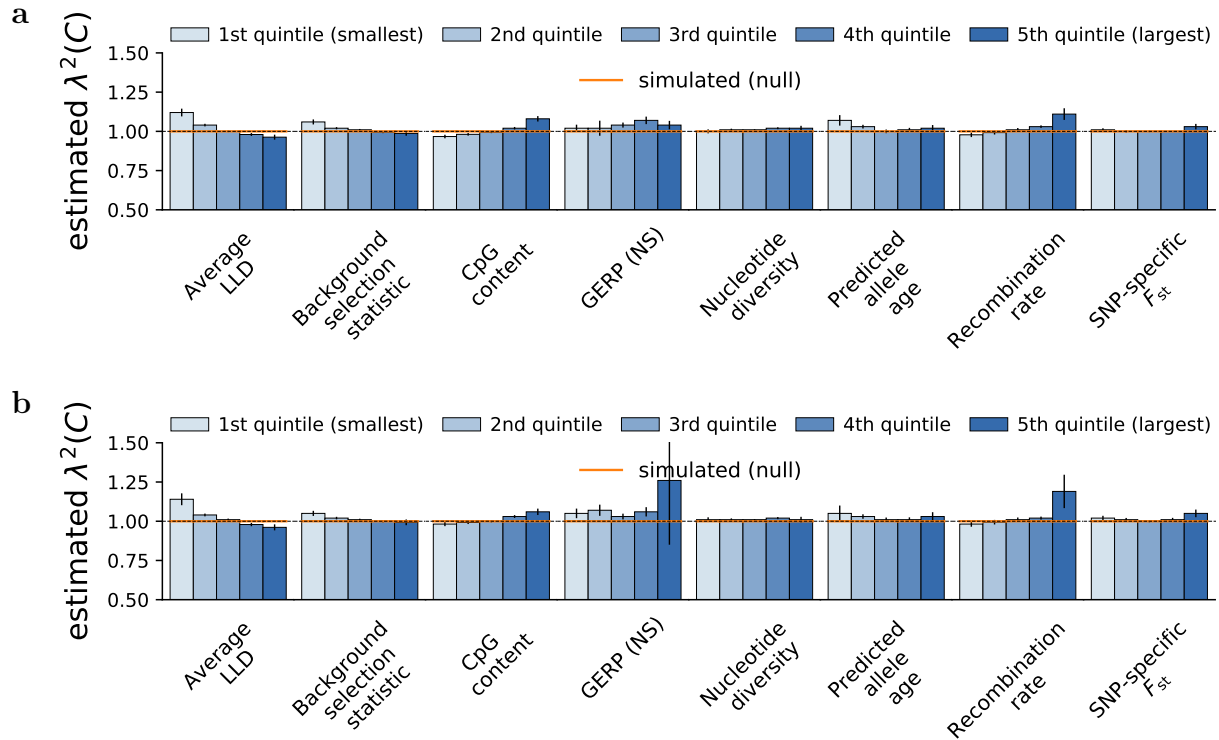
Supplementary Figure 7: (continued on next page)



Supplementary Figure 7: **Q-Q plot for S-LDXR p-values testing enrichment of squared trans-ethnic genetic correlation of 20 main functional annotations in 1,000 null simulations.** 10% of SNPs were randomly selected to be causal. S-LDXR was applied with the baseline-LD-X model annotations. The shrinkage level,  $\alpha$ , was set to 0.5. Here, the p-values are unadjusted two-tailed p-values obtained from a t distribution with 44 (number of jackknife blocks  $- 1$ ) degrees of freedom. Shaded area represent the 95% confidence interval around the mean. Size of the annotation (proportion of SNPs) is shown in parentheses.

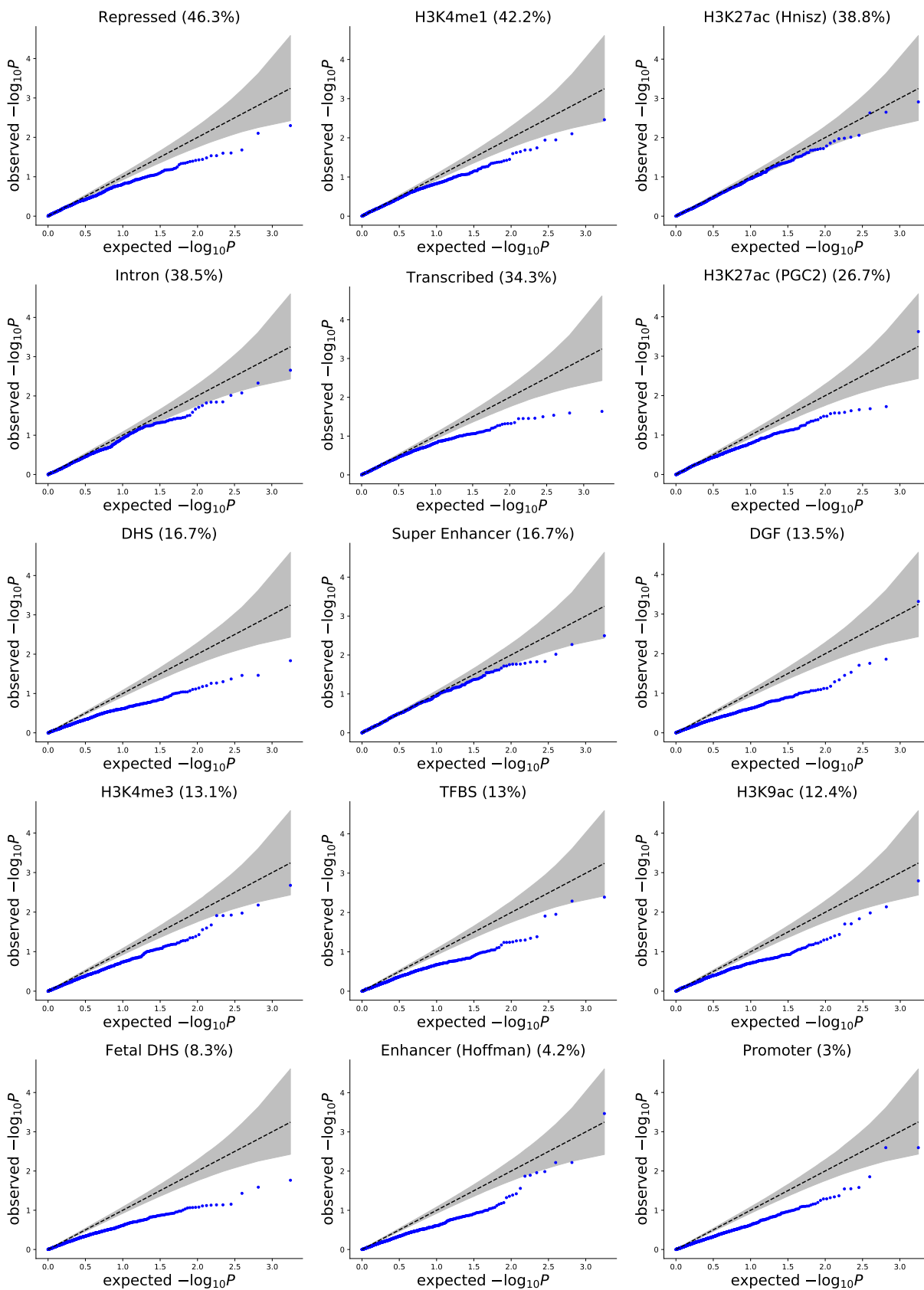


Supplementary Figure 8: **Accuracy of S-LDXR in estimating enrichment of stratified squared trans-ethnic genetic correlation,  $\lambda^2(C)$ , of functional annotations in simulations with annotation-dependent MAF-dependent genetic architectures.** 10% of SNPs were randomly selected to be causal. Shrinkage level,  $\alpha$ , was set to 0.5. **a)** S-LDXR was applied with the baseline-LD-X model annotations. **b)** S-LDXR was applied with the baseline-LD-X model annotations and 5 MAF bin annotations. Mean and standard errors were obtained across 1,000 simulations. Error bars represent 1.96 times the standard error on both sides.

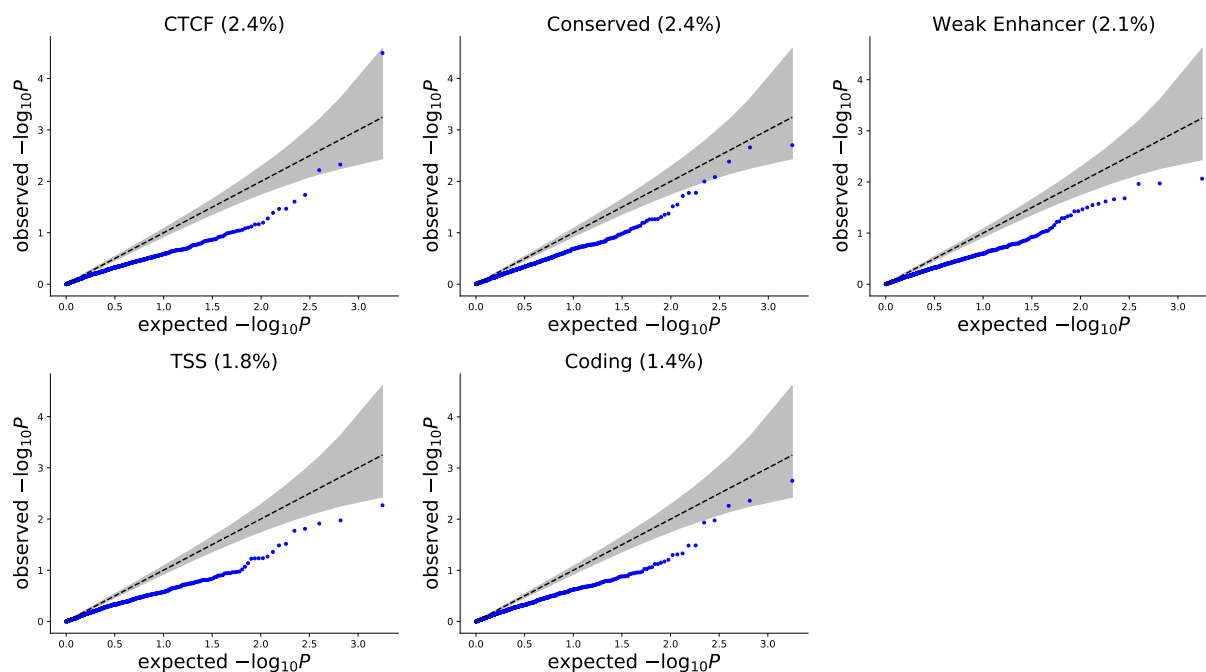


Supplementary Figure 9: **Accuracy of S-LDXR in estimating enrichment of stratified squared trans-ethnic genetic correlation,  $\lambda^2(C)$ , of quintiles of continuous-valued annotations in simulations with annotation-dependent MAF-dependent genetic architectures.** 10% of SNPs were randomly selected to be causal. Shrinkage level,  $\alpha$ , was set to 0.5. **a)** S-LDXR was applied with the baseline-LD-X model annotations. **b)** S-LDXR was applied with the baseline-LD-X model annotations and 5 MAF bin annotations. Mean and standard errors were obtained across 1,000 simulations. Error bars represent 1.96 times the standard error on both sides.

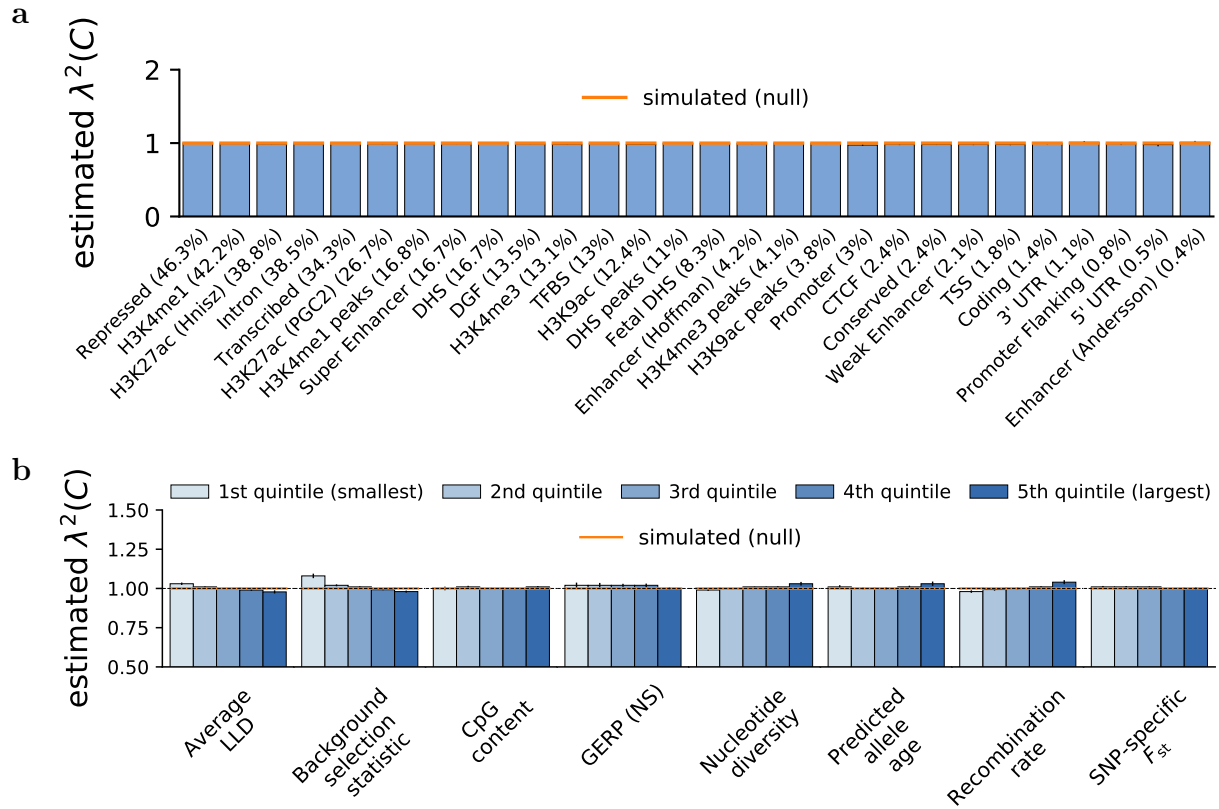




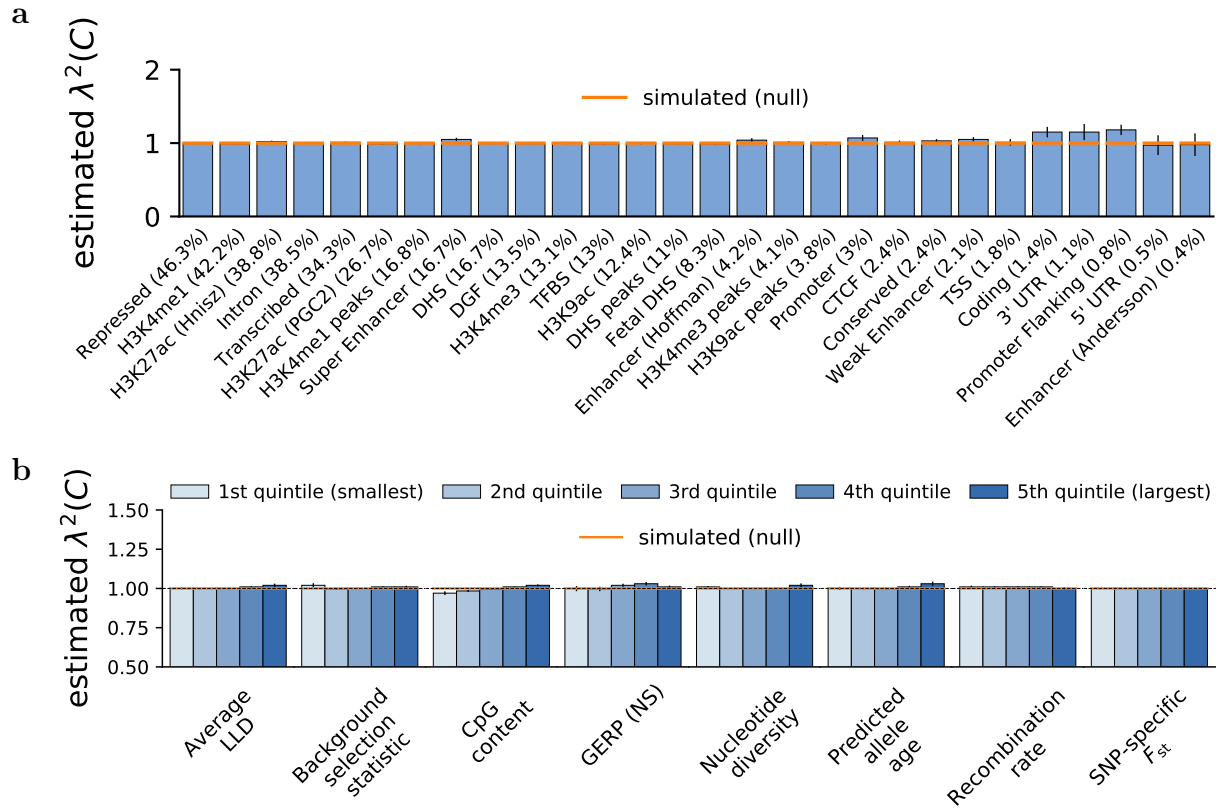
Supplementary Figure 10: (continued on next page)



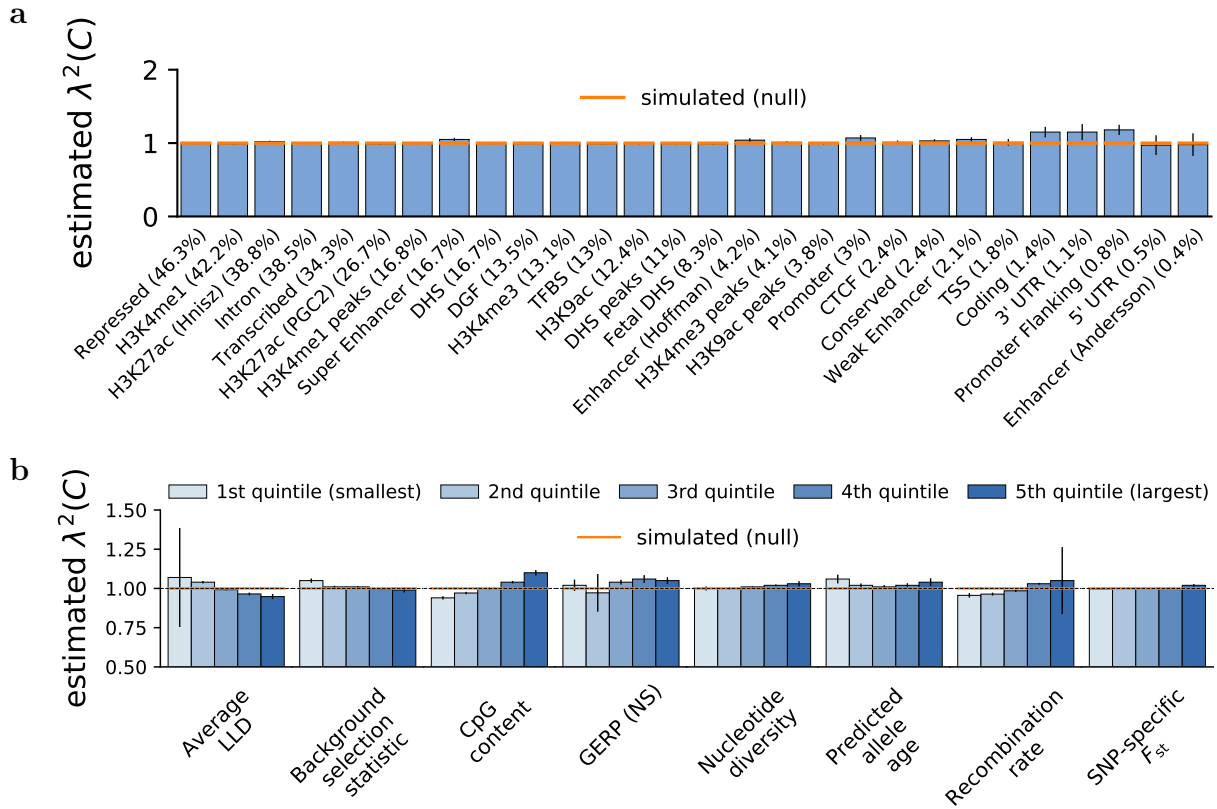
Supplementary Figure 10: **Q-Q plot for S-LDXR p-values testing enrichment of squared trans-ethnic genetic correlation of 20 main functional annotations in 1,000 null simulations with annotation-dependent MAF-dependent genetic architectures.** 10% of SNPs were randomly selected to be causal. S-LDXR was applied with the baseline-LD-X model annotations. The shrinkage level,  $\alpha$ , was set to 0.5. Here, the p-values are unadjusted two-tailed p-values obtained from a t distribution with 44 (number of jackknife blocks – 1) degrees of freedom. Shaded area represent the 95% confidence interval around the mean. Size of the annotation (proportion of SNPs) is shown in parenthesis.



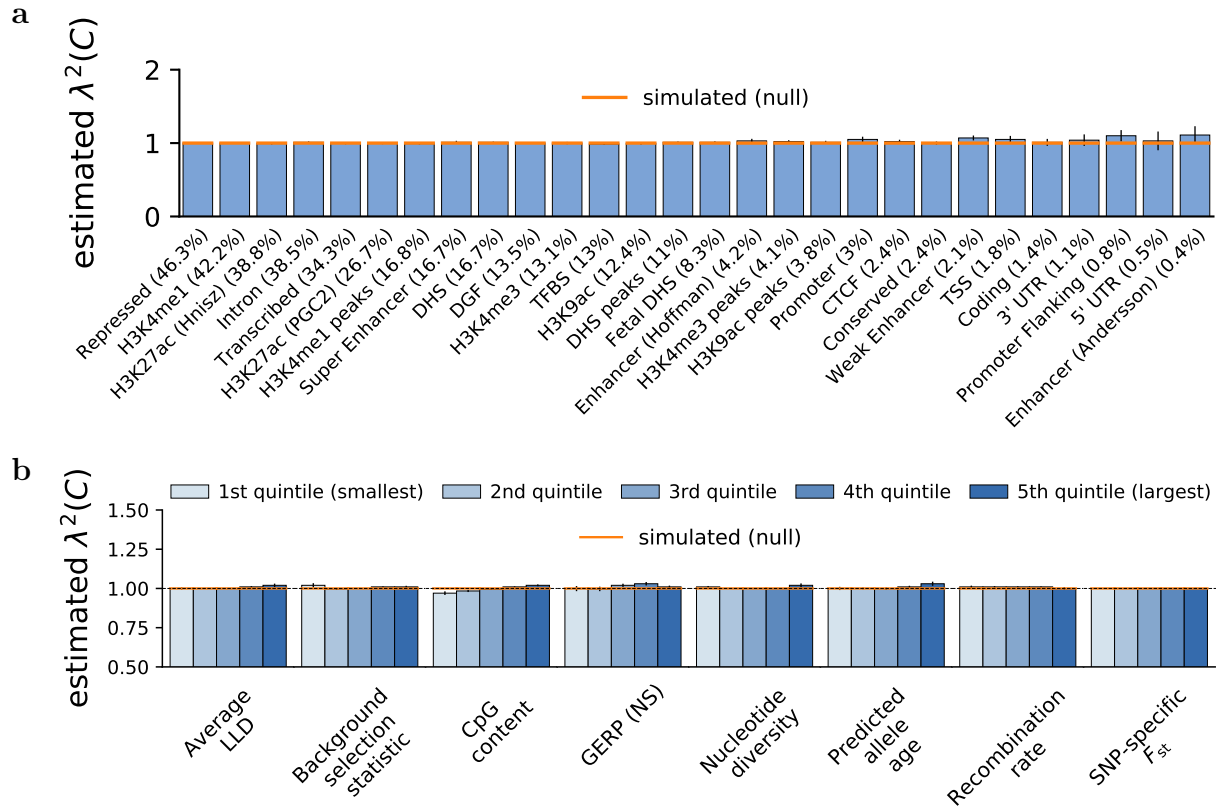
Supplementary Figure 11: **Accuracy of S-LDXR in estimating enrichment of stratified squared trans-ethnic genetic correlation,  $\lambda^2(C)$ , when causal variants differ across the two populations.** 10% of SNPs were randomly selected to be causal. Shrinkage level,  $\alpha$ , was set to 0.5. **a)** Estimates of  $\lambda^2(C)$  for binary functional annotations. **b)** Estimates of  $\lambda^2(C)$  for quintiles of continuous-valued annotations. Mean and standard errors were obtained across 1,000 simulations. Error bars represent 1.96 times the standard error on both sides.



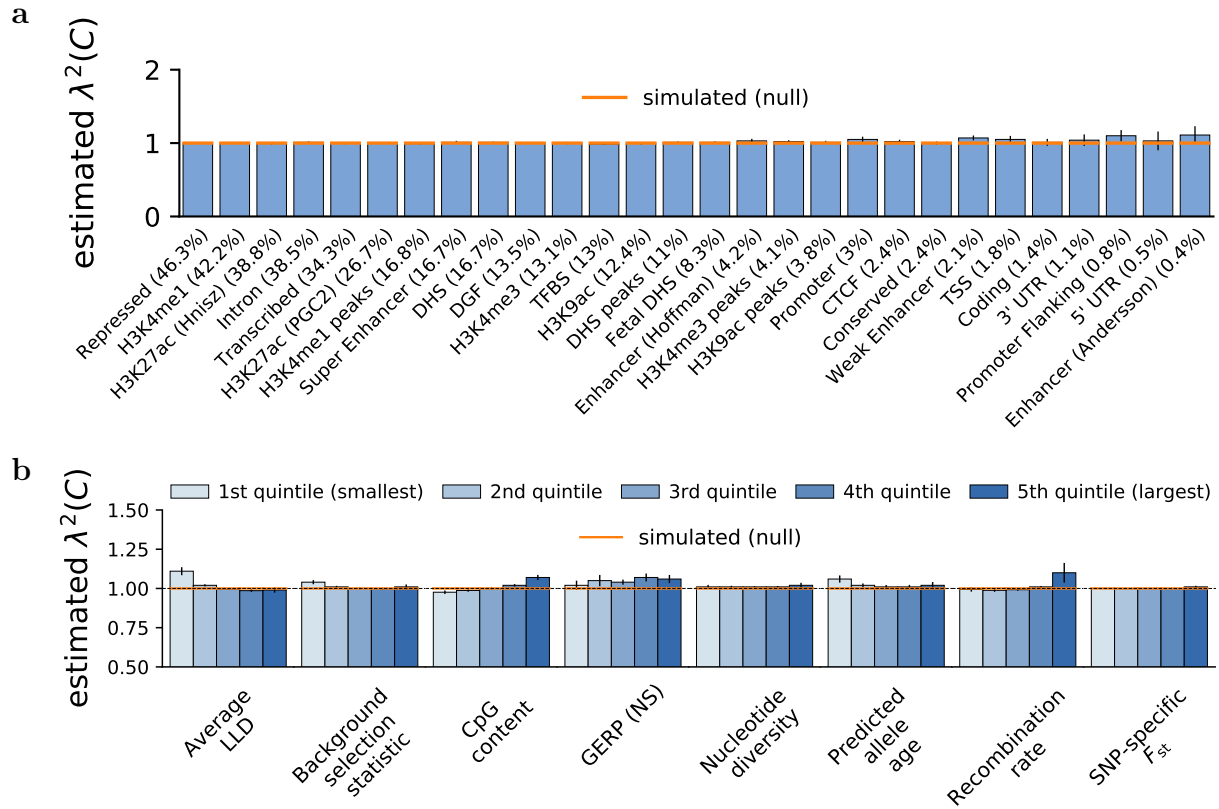
Supplementary Figure 12: **Accuracy of S-LDXR in estimating enrichment of stratified squared trans-ethnic genetic correlation,  $\lambda^2(C)$ , in simulations under the baseline-LD-X model using all simulated GWAS samples and half (250) the default reference panel sample size.** 10% of SNPs were randomly selected to be causal. Shrinkage level,  $\alpha$ , was set to 0.5. **a)** Estimates of  $\lambda^2(C)$  for binary functional annotations. **b)** Estimates of  $\lambda^2(C)$  for quintiles of continuous-valued annotations. Mean and standard errors were obtained across 1,000 simulations. Error bars represent 1.96 times the standard error on both sides. Numerical results are reported in Supplementary Data 12a.



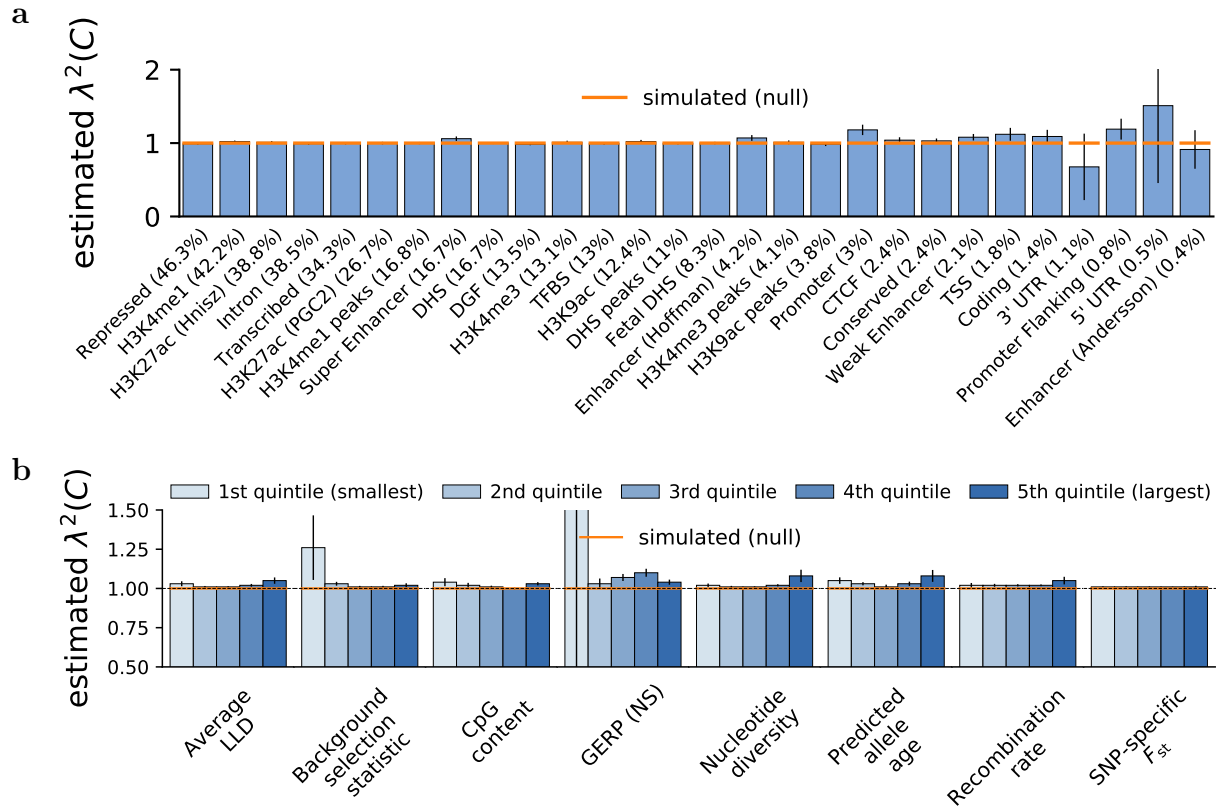
Supplementary Figure 13: **Accuracy of S-LDXR in estimating enrichment of stratified squared trans-ethnic genetic correlation,  $\lambda^2(C)$ , in simulations with annotation-dependent MAF-dependent genetic architectures using all simulated GWAS samples and half (250) the default reference panel sample size.** 10% of SNPs were randomly selected to be causal. Shrinkage level,  $\alpha$ , was set to 0.5. **a)** Estimates of  $\lambda^2(C)$  for binary functional annotations. **b)** Estimates of  $\lambda^2(C)$  for quintiles of continuous-valued annotations. Mean and standard errors were obtained across 1,000 simulations. Error bars represent 1.96 times the standard error on both sides. Numerical results are reported in Supplementary Data 12b.



Supplementary Figure 14: **Accuracy of S-LDXR in estimating enrichment of stratified squared trans-ethnic genetic correlation,  $\lambda^2(C)$ , in simulations under the baseline-LD-X model using all simulated GWAS samples and twice (1,000) the default reference panel sample size.** 10% of SNPs were randomly selected to be causal. Shrinkage level,  $\alpha$ , was set to 0.5. **a)** Estimates of  $\lambda^2(C)$  for binary functional annotations. **b)** Estimates of  $\lambda^2(C)$  for quintiles of continuous-valued annotations. Mean and standard errors were obtained across 1,000 simulations. Error bars represent 1.96 times the standard error on both sides. Numerical results are reported in Supplementary Data 13a.

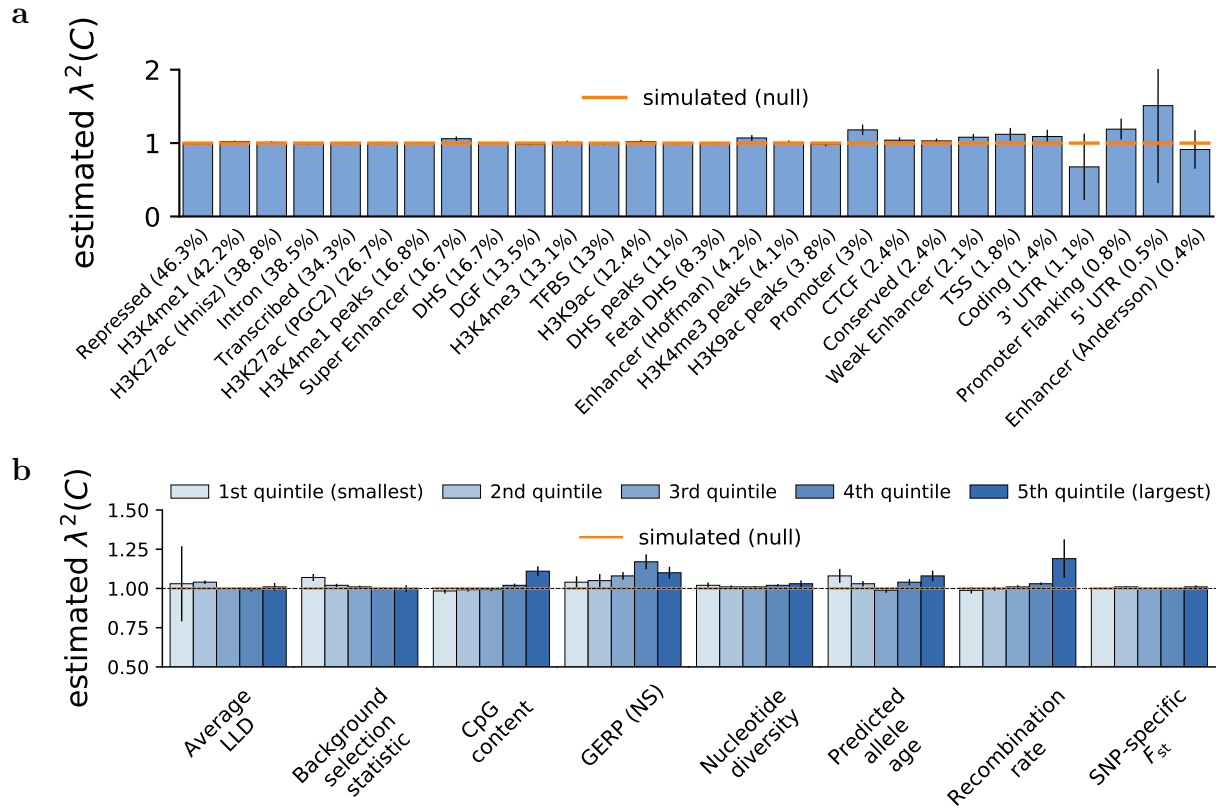


Supplementary Figure 15: **Accuracy of S-LDXR in estimating enrichment of stratified squared trans-ethnic genetic correlation,  $\lambda^2(C)$ , in simulations with annotation-dependent MAF-dependent genetic architectures using all simulated GWAS samples and twice (1,000) the default reference panel sample size.** 10% of SNPs were randomly selected to be causal. Shrinkage level,  $\alpha$ , was set to 0.5. **a)** Estimates of  $\lambda^2(C)$  for binary functional annotations. **b)** Estimates of  $\lambda^2(C)$  for quintiles of continuous-valued annotations. Mean and standard errors were obtained across 1,000 simulations. Error bars represent 1.96 times the standard error on both sides. Numerical results are reported in Supplementary Data 13b.

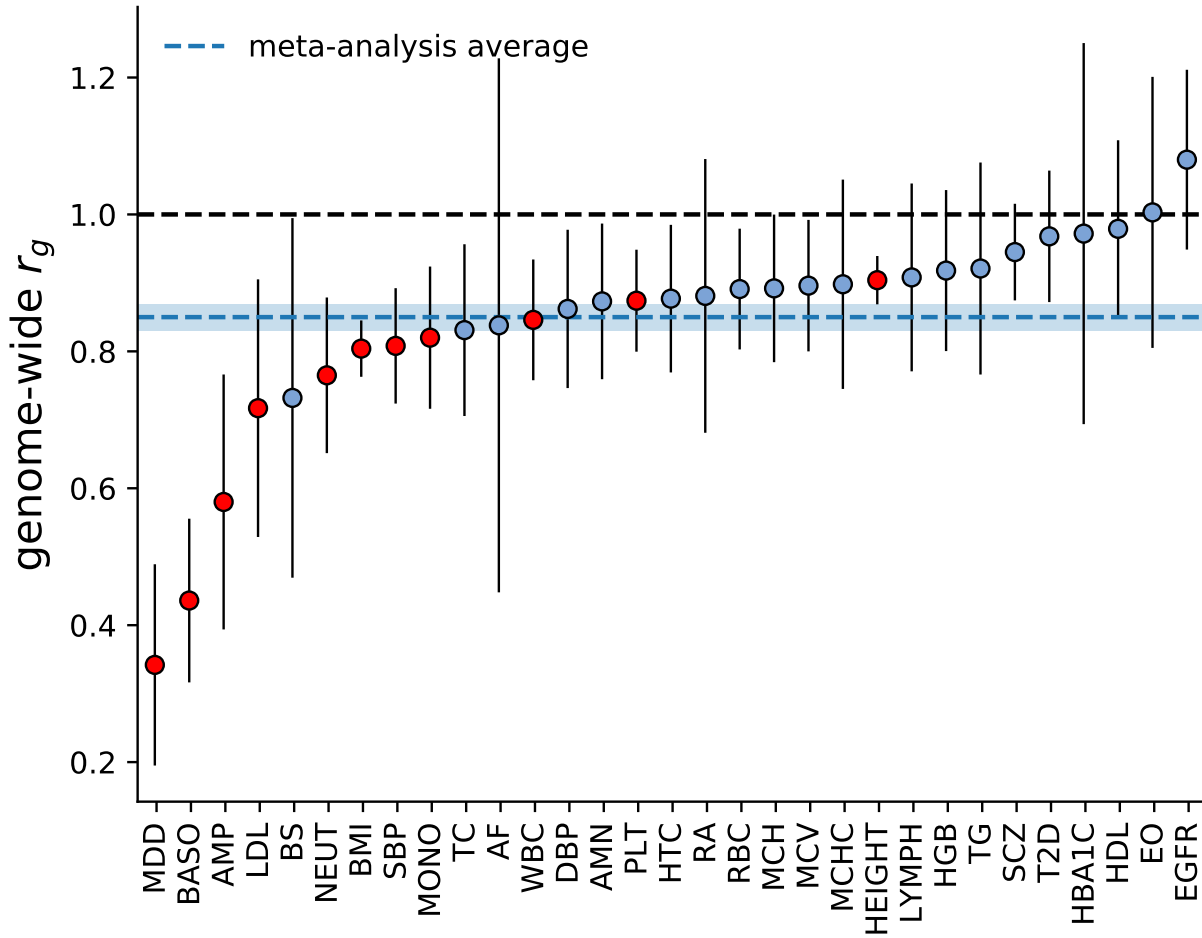


Supplementary Figure 16: **Accuracy of S-LDXR in estimating enrichment of stratified squared trans-ethnic genetic correlation,  $\lambda^2(C)$ , in simulations under the baseline-LD-X model using half of the simulated GWAS samples and the default (500) reference panel sample size.** 10% of SNPs were randomly selected to be causal. Shrinkage level,  $\alpha$ , was set to 0.5. **a)** Estimates of  $\lambda^2(C)$  for binary functional annotations. **b)** Estimates of  $\lambda^2(C)$  for quintiles of continuous-valued annotations. Mean and standard errors were obtained across 1,000 simulations. Error bars represent 1.96 times the standard error on both sides. Numerical results are reported in Supplementary Data 14a.

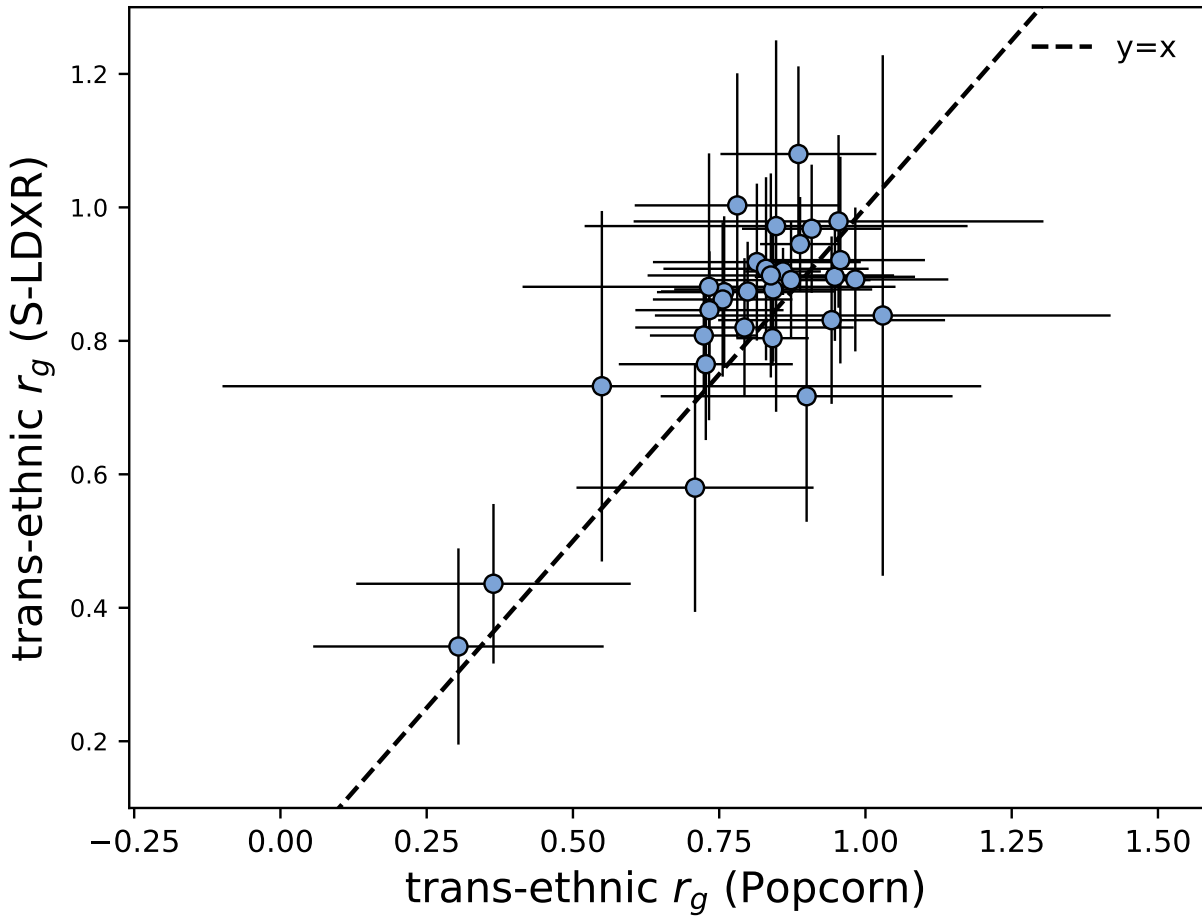




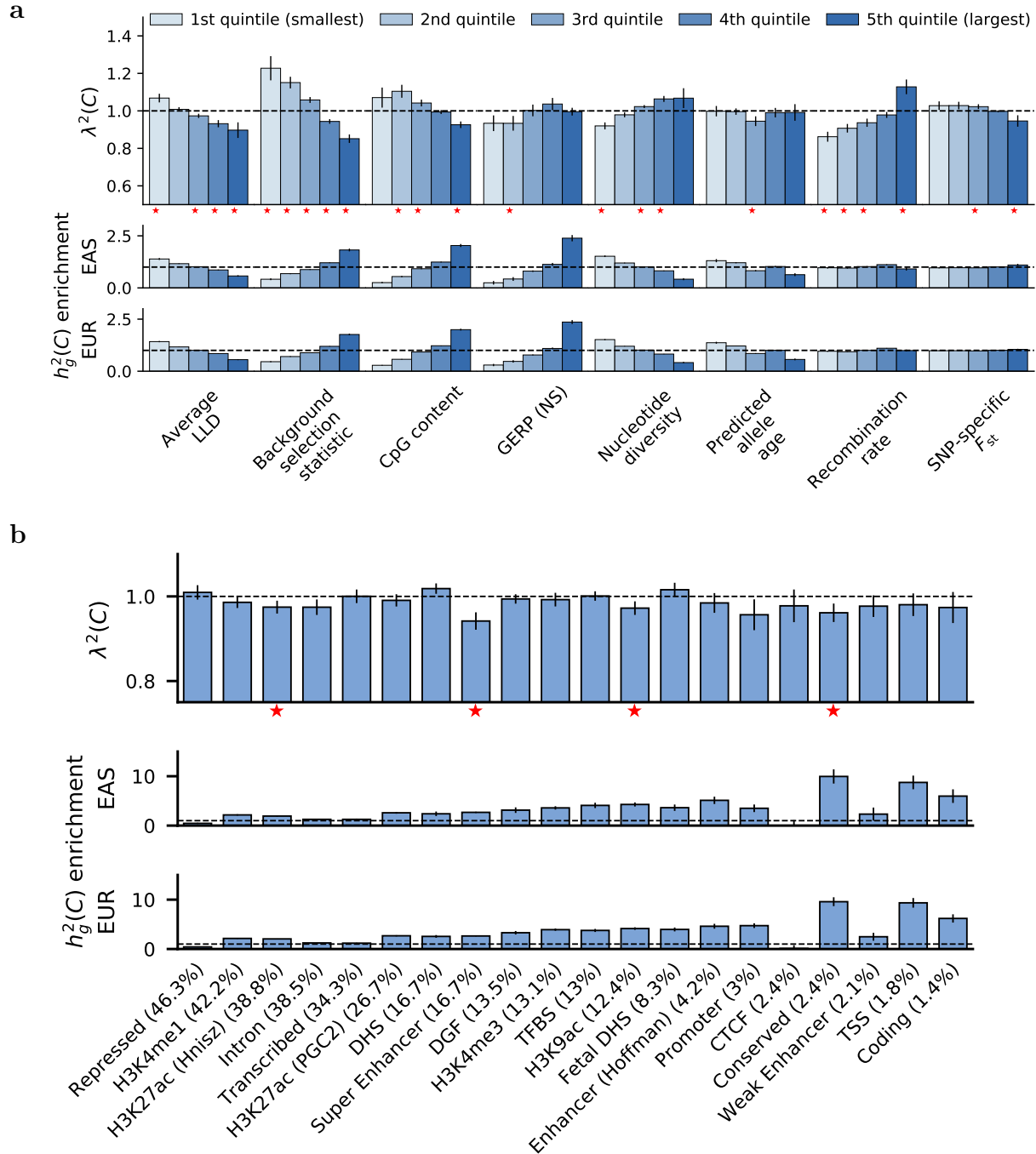
Supplementary Figure 17: **Accuracy of S-LDXR in estimating enrichment of stratified squared trans-ethnic genetic correlation,  $\lambda^2(C)$ , in simulations with annotation-dependent MAF-dependent genetic architectures using half of the simulated GWAS samples and the default (500) reference panel sample size.** 10% of SNPs were randomly selected to be causal. Shrinkage level,  $\alpha$ , was set to 0.5. **a)** Estimates of  $\lambda^2(C)$  for binary functional annotations. **b)** Estimates of  $\lambda^2(C)$  for quintiles of continuous-valued annotations. Mean and standard errors were obtained across 1,000 simulations. Error bars represent 1.96 times the standard error on both sides. Numerical results are reported in Supplementary Data 14b.



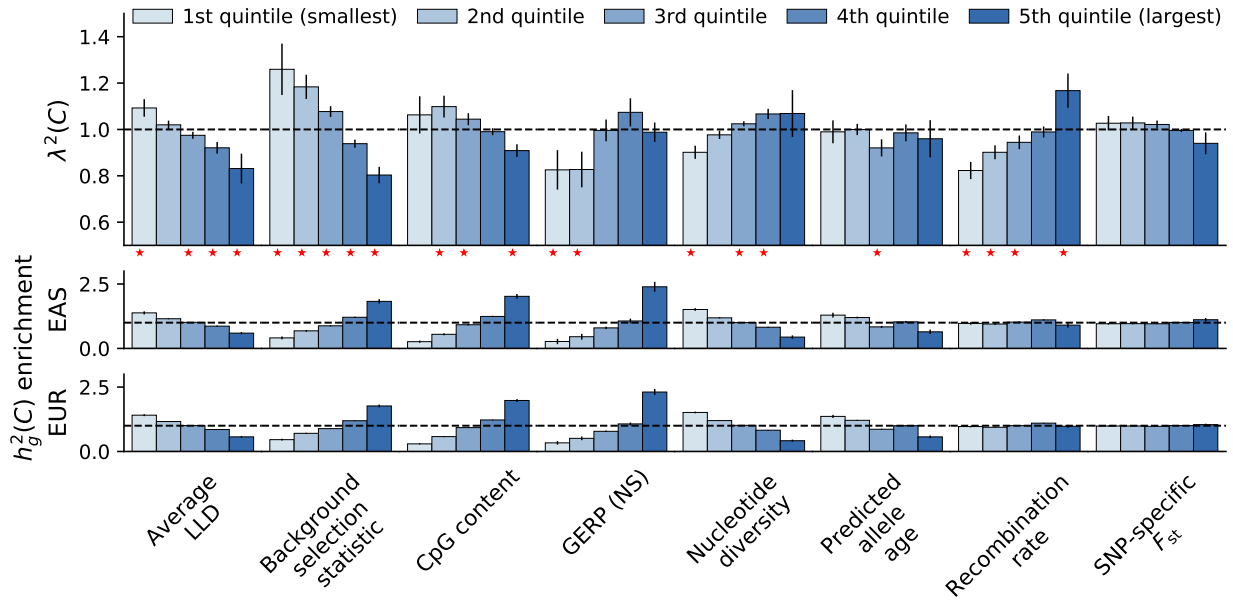
Supplementary Figure 18: **Genome-wide trans-ethnic genetic correlation for 31 diseases and complex traits.** Diseases and complex traits are sorted by the magnitude of trans-ethnic genetic correlation. Traits with estimated trans-ethnic genetic correlation significantly less than 1 (one-tailed  $p < 0.05/31$ ) are marked by red filled dots. Here, p-values are obtained from the t distribution with 199 (number of jackknife blocks – 1) degrees of freedom. Full name of the traits can be found in Supplementary Table 2. Error bars represent  $\pm 1.96 \times$  the jackknife standard error of the estimated genome-wide trans-ethnic genetic correlation. The blue dashed line represents meta-analyzed  $r_g$ , and the shaded region covers 1.96 times the meta-analysis standard error on each side.



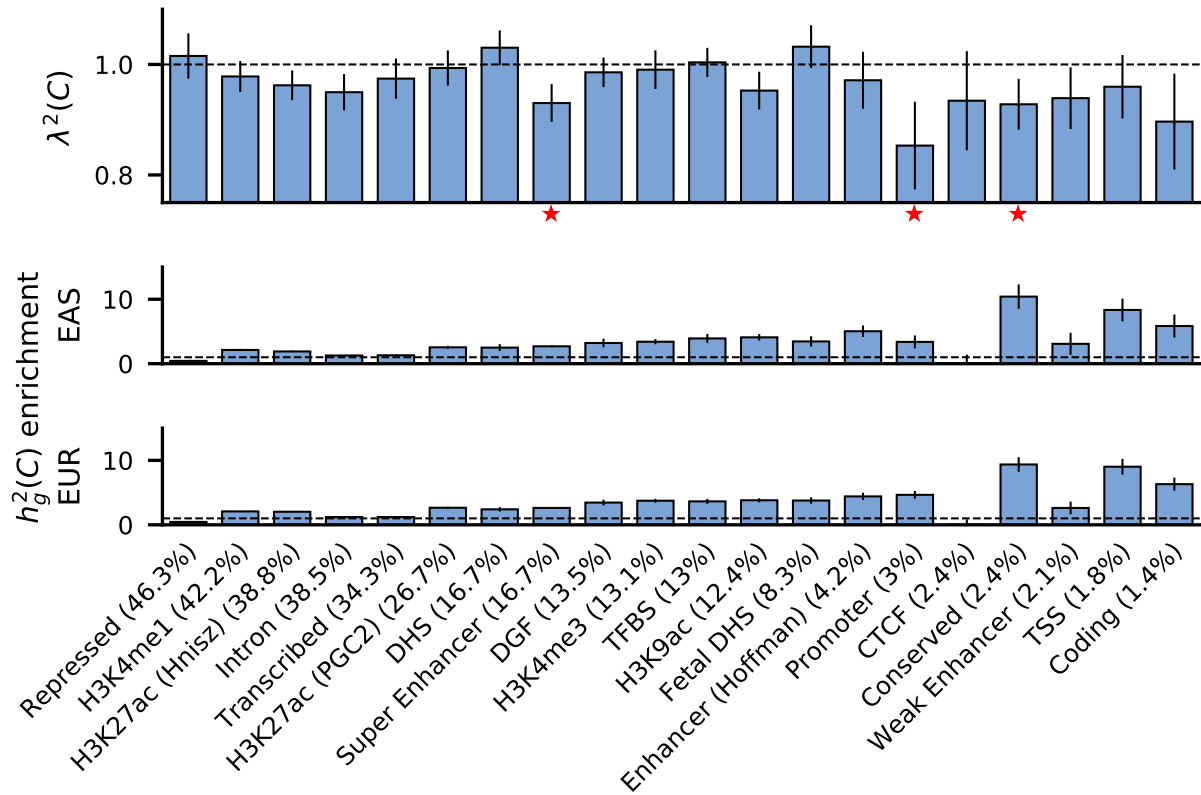
Supplementary Figure 19: **Comparison of S-LDXR vs. Popcorn<sup>2</sup> estimates of genome-wide trans-ethnic genetic correlations for 31 diseases and complex traits.** Error bars represent  $\pm 1.96 \times$  the jackknife standard error of the estimated genome-wide trans-ethnic genetic correlation. The meta-analyze average  $r_g$  of S-LDXR and Popcorn are 0.85 (s.e. 0.01) and 0.82 (s.e. 0.01), respectively.



Supplementary Figure 20: **Enrichment of stratified squared trans-ethnic genetic correlation,  $\lambda^2(C)$ , across 31 diseases and complex traits, across a) quintiles of continuous-valued annotations and b) functional annotations.** The shrinkage level,  $\alpha$ , was set to 1.0. Error bars represent  $\pm 1.96 \times$  the standard error of the meta-analyzed  $\lambda^2(C)$ . P-values are obtained from a standard normal distribution. Red stars ( $\star$ ) denote two-tailed  $p < 0.05/20$ .

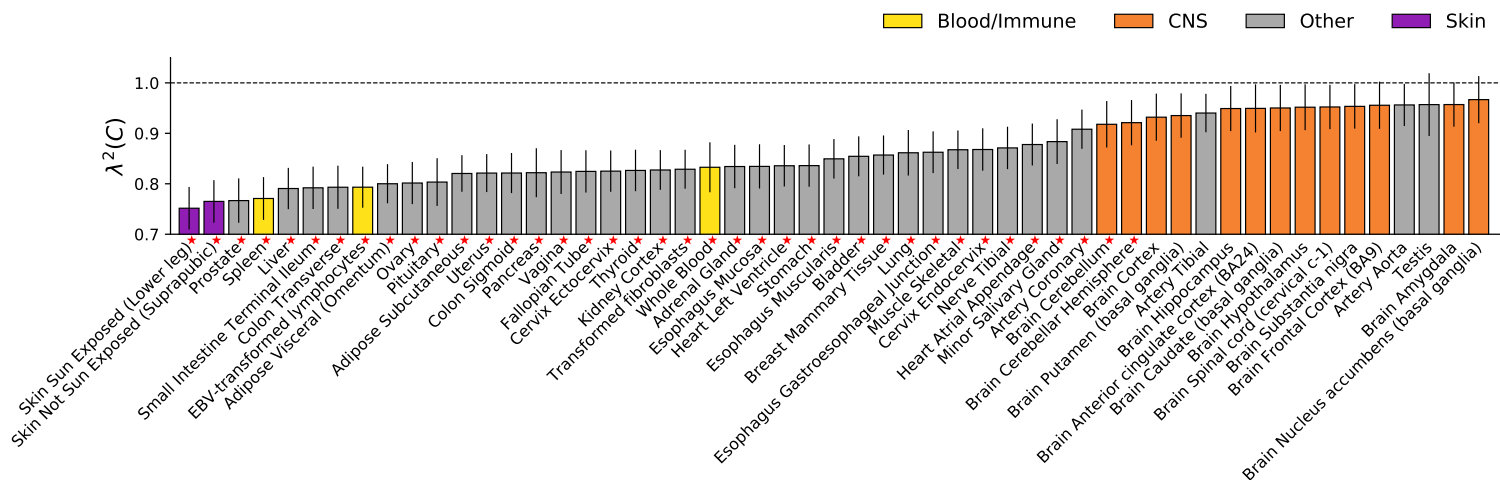


Supplementary Figure 21: **S-LDXR results for quintiles of 8 continuous-valued annotations across 20 approximately independent diseases and complex traits.** The shrinkage parameter,  $\alpha$ , was set to 0.5. Error bars represent  $\pm 1.96 \times$  the standard error of the meta-analyzed  $\lambda^2(C)$ . P-values are obtained from a standard normal distribution. Red stars (\*) denote two-tailed  $p < 0.05/40$ .

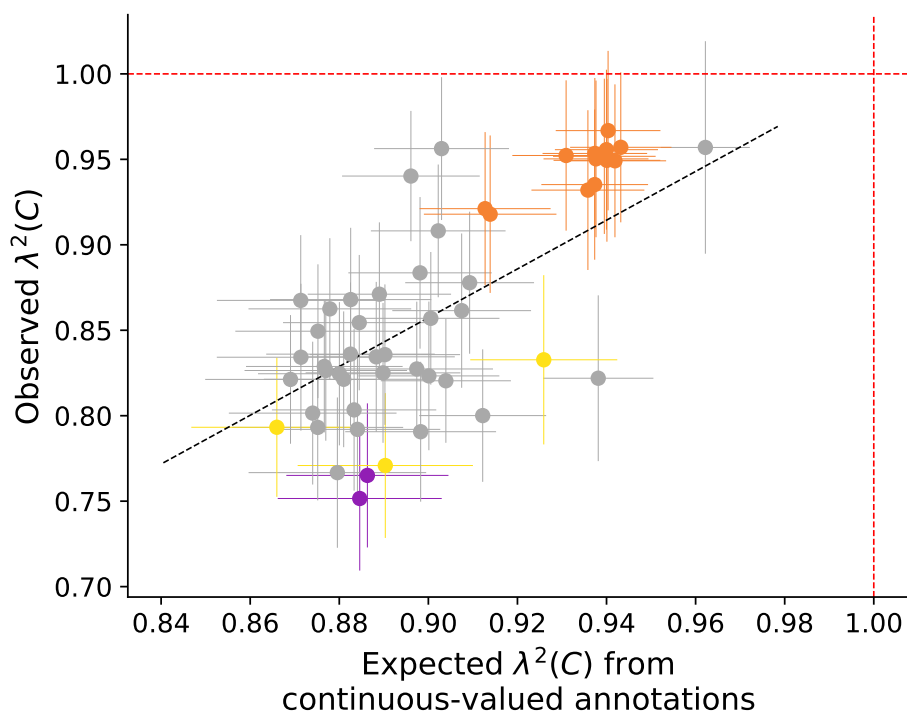


Supplementary Figure 22: **S-LDXR results for 20 binary functional annotations across 20 approximately independent diseases and complex traits.** The shrinkage parameter,  $\alpha$ , was set to 0.5. Error bars represent  $\pm 1.96 \times$  the standard error of the meta-analyzed  $\lambda^2(C)$ . P-values are obtained from a standard normal distribution. Red stars (\*) denote two-tailed  $p < 0.05/20$ .

a

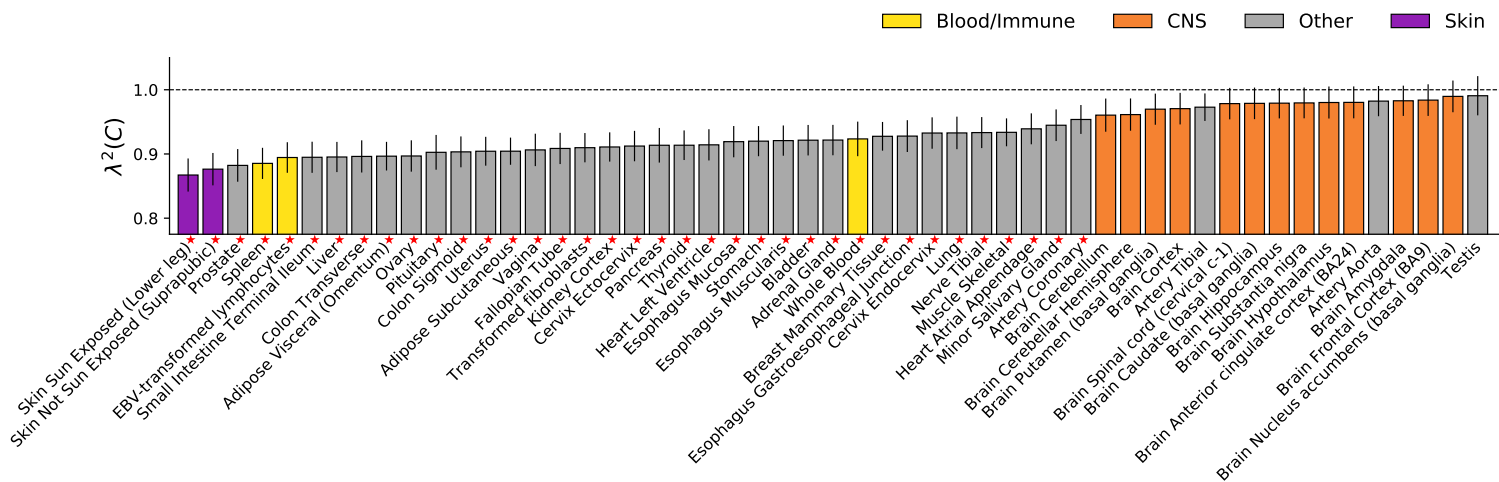


b

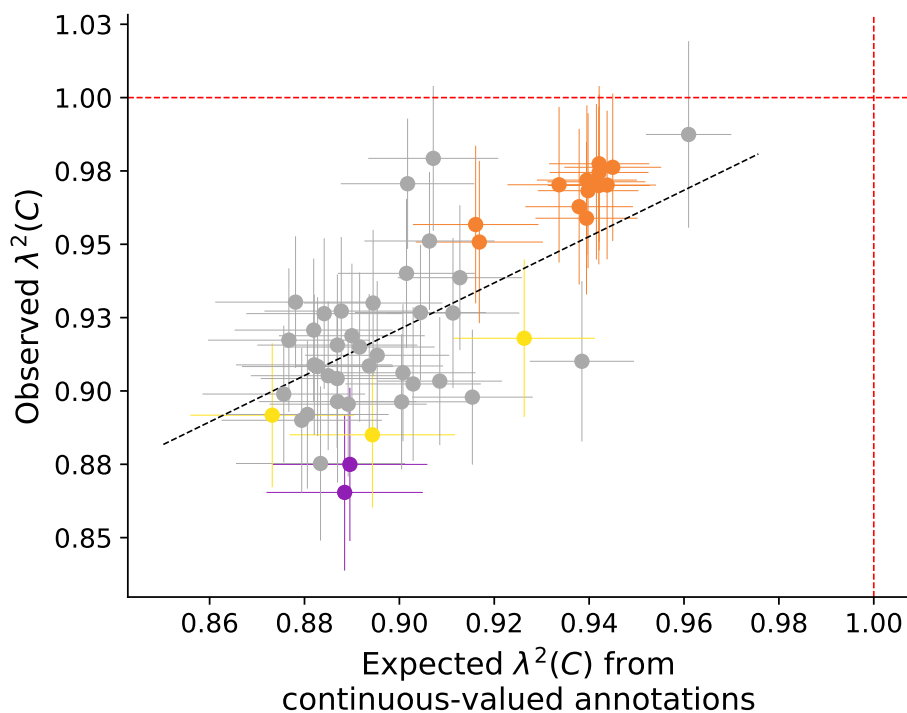


Supplementary Figure 23: **S-LDXR results for 53 specifically expressed gene (SEG) annotations across 31 diseases and complex traits in analyses with the shrinkage parameter  $\alpha$  set to 0.0.** (a) We report estimates of the enrichment/depletion of squared trans-ethnic genetic correlation ( $\lambda^2(C)$ ) for each SEG annotation (sorted by  $\lambda^2(C)$ ). Results are meta-analyzed across 31 diseases and complex traits. Error bars denote  $\pm 1.96 \times$  the standard error of the meta-analyzed  $\lambda^2(C)$ . P-values are obtained from the standard normal distribution. Red stars ( $\star$ ) denote two-tailed  $p < 0.05/53$ . Numerical results are reported in Supplementary Data 20. (b) We report observed  $\lambda^2(C)$  vs. expected  $\lambda^2(C)$  based on 8 continuous-valued annotations, for each SEG annotation. Results are meta-analyzed across 31 diseases and complex traits. Error bars denote  $\pm 1.96 \times$  standard error. Annotations are color-coded as in (a). The dashed black line (slope=1.40) denotes a regression of observed  $\lambda(C) - 1$  vs. expected  $\lambda(C) - 1$  with intercept ( $R = 0.74$ ) constrained to 0. Numerical results including population-specific heritability enrichment estimates are reported in Supplementary Data 20.

a

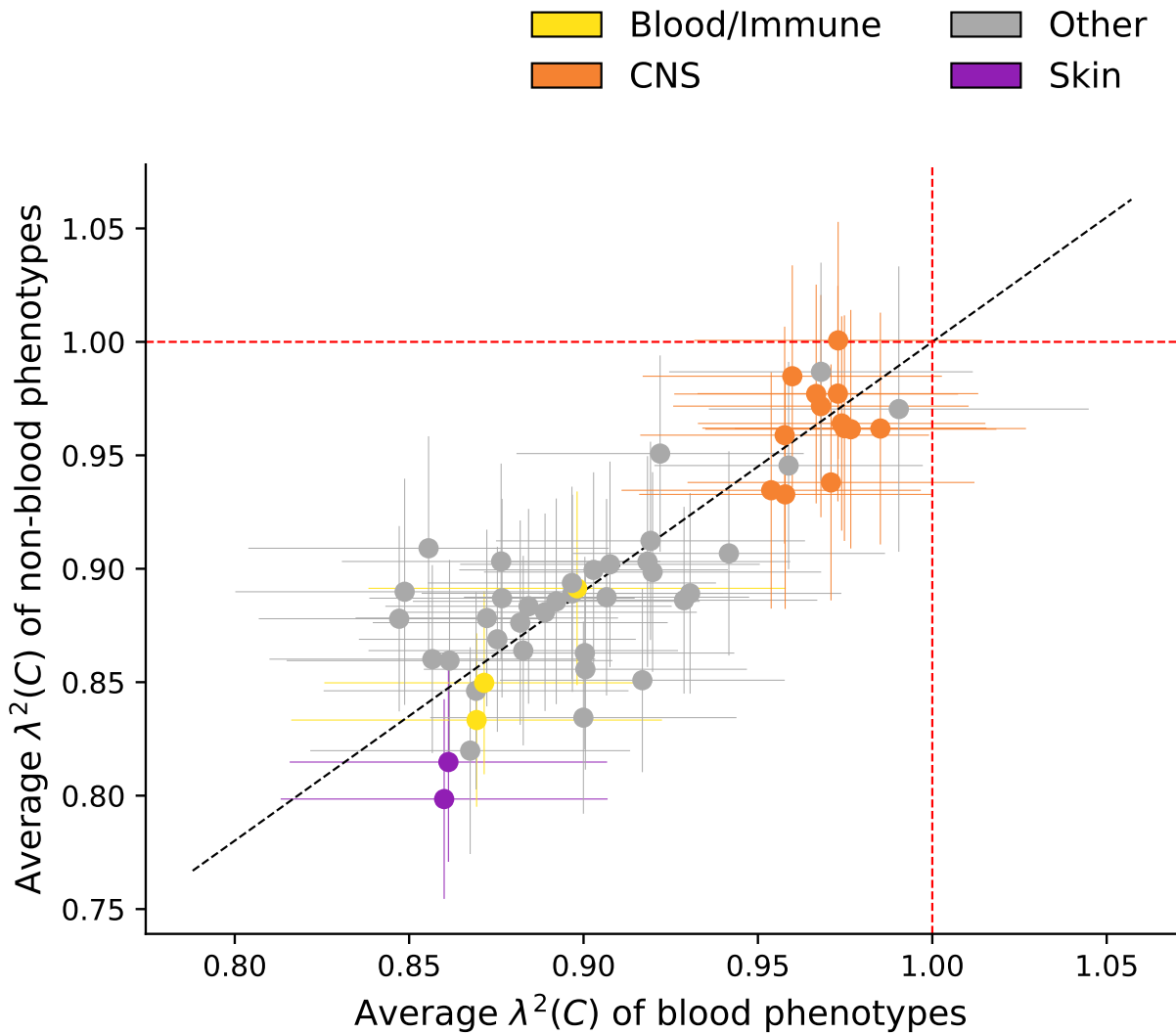


b



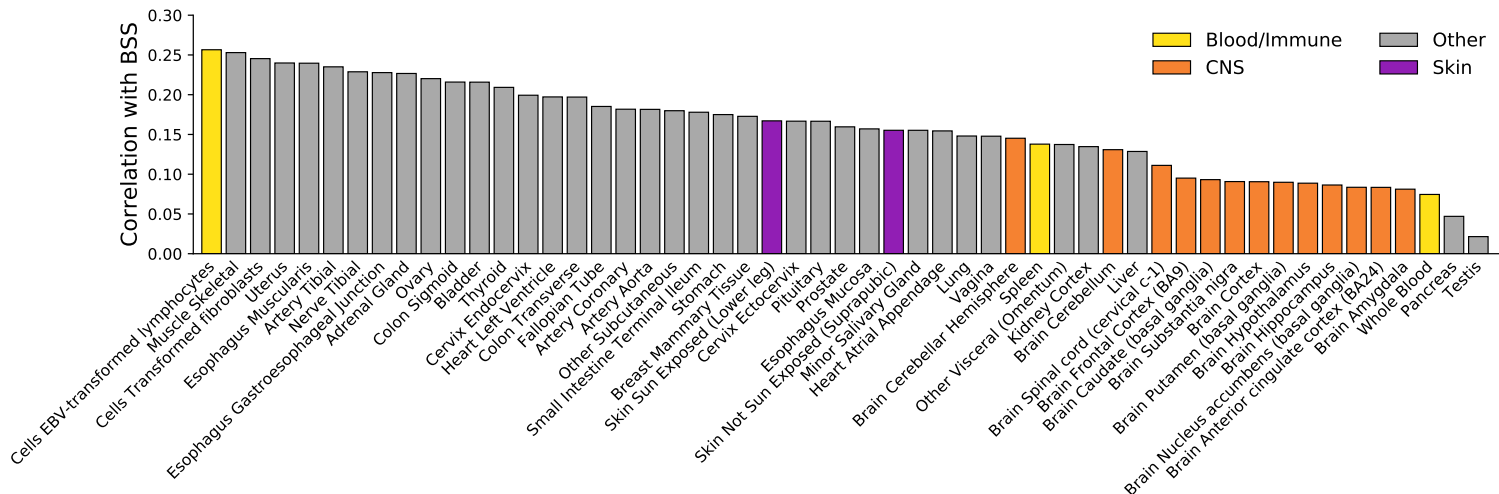
Supplementary Figure 24: **S-LDXR results for 53 specifically expressed gene (SEG) annotations across 31 diseases and complex traits in analyses with the shrinkage parameter  $\alpha$  set to 1.0.** (a) We report estimates of the enrichment/depletion of squared trans-ethnic genetic correlation ( $\lambda^2(C)$ ) for each SEG annotation (sorted by  $\lambda^2(C)$ ). Results are meta-analyzed across 31 diseases and complex traits. Error bars denote  $\pm 1.96 \times$  the standard error of the meta-analyzed  $\lambda^2(C)$ . P-values are obtained from the standard normal distribution. Red stars ( $\star$ ) denote two-tailed  $p < 0.05/53$ . Numerical results are reported in Supplementary Data 18. (b) We report observed  $\lambda^2(C)$  vs. expected  $\lambda^2(C)$  based on 8 continuous-valued annotations, for each SEG annotation. Results are meta-analyzed across 31 diseases and complex traits. Error bars denote  $\pm 1.96 \times$  standard error. Annotations are color-coded as in (a). The dashed black line (slope=0.76) denotes a regression of observed  $\lambda(C) - 1$  vs. expected  $\lambda(C) - 1$  ( $R = 0.76$ ) with intercept constrained to 0. Numerical results including population-specific heritability enrichment estimates are reported in Supplementary Data 20.



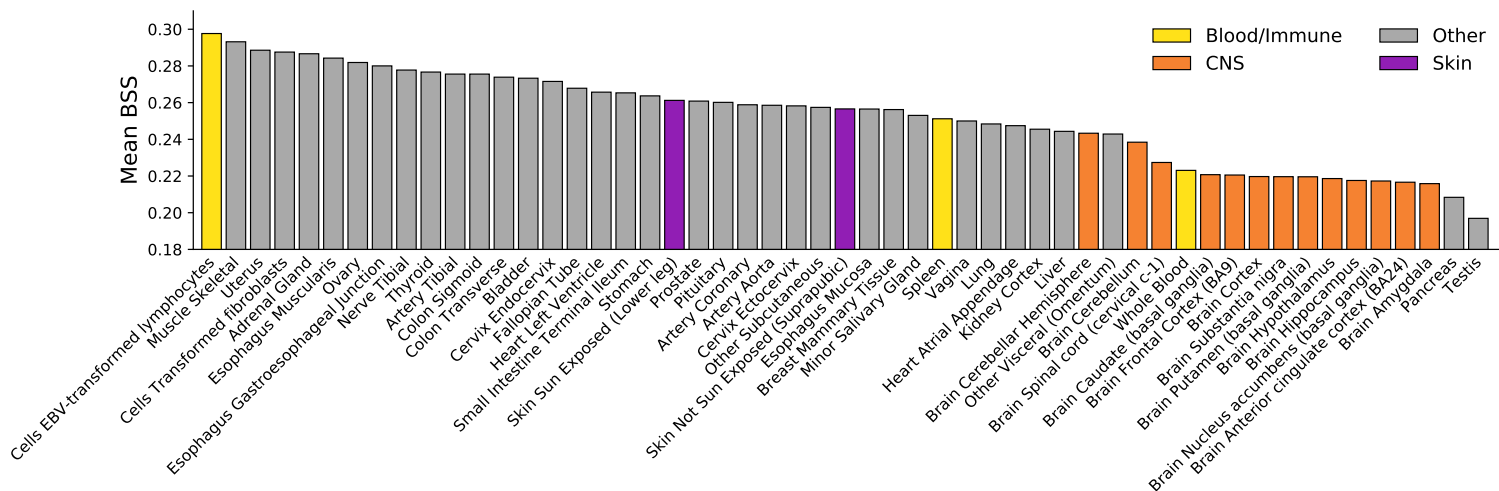


Supplementary Figure 25: **Comparison of S-LDXR results for 53 specifically expressed gene (SEG) annotations for 14 blood-related traits vs. 17 other traits.** The list of 14 blood phenotypes is: BASO, EO, HBA1C, HGB, HTC, LYMPH, MCH, MCHC, MCV, MONO, NEUT, PLT, RBC, WBC. The list of 16 non-blood phenotype is: AF, AMN, AMP, BMI, BS, DBP, EGFR, HEIGHT, HDL, LDL, MDD, RA, SBP, SCZ, TC, TG, T2D. Full name of the abbreviations can be found in Supplementary Table 2. Here, the shrinkage parameter was set to 0.5. Error bars denote  $\pm 1.96 \times$  the standard error of the meta-analyzed  $\lambda^2(C)$ . The black dashed line represent the regression line (slope=1.10) fitting  $(\lambda^2(C) - 1)$  of non-blood phenotypes and  $(\lambda^2(C) - 1)$  of blood phenotypes, with intercept constrained to 0.

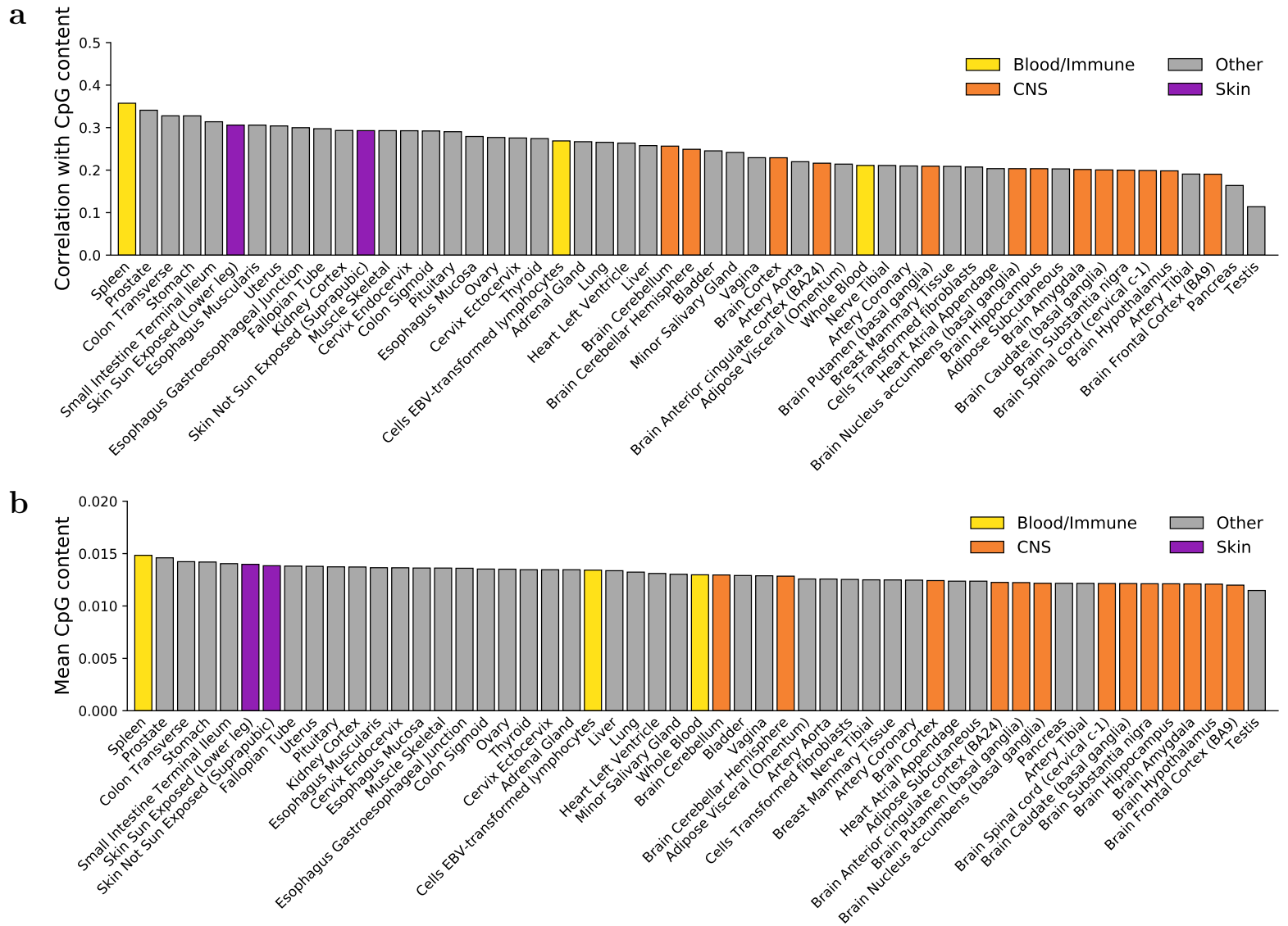
a



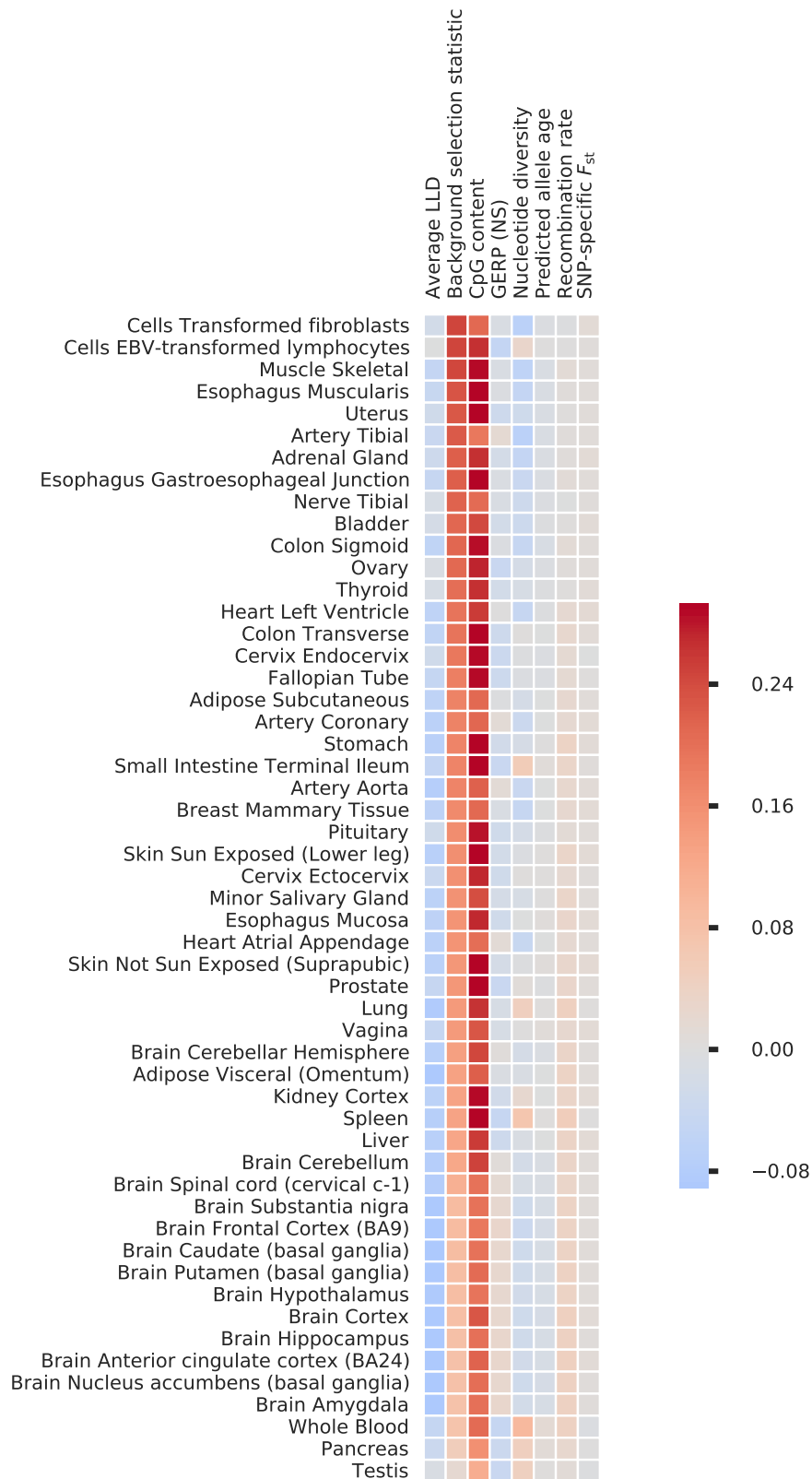
b



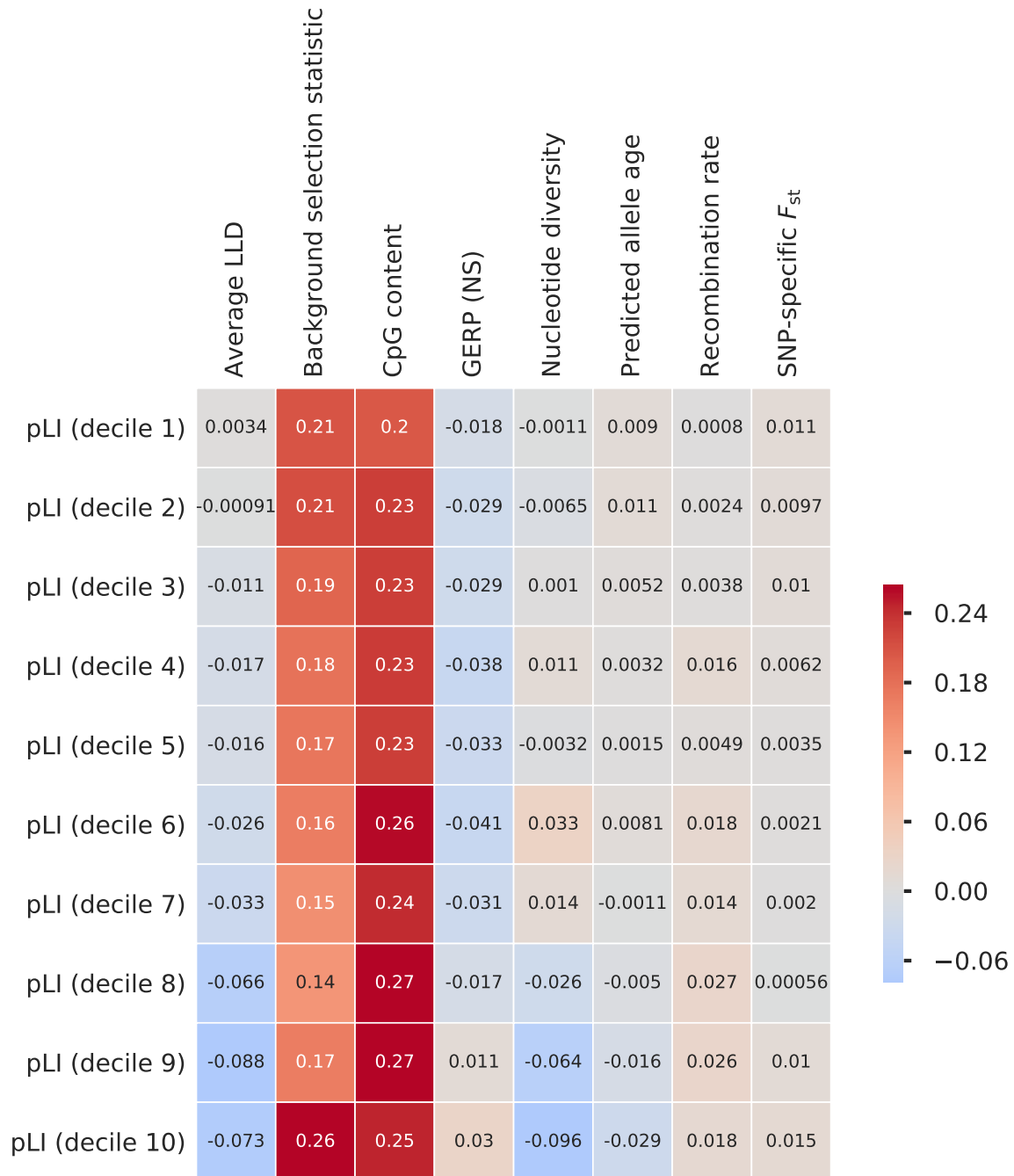
Supplementary Figure 26: **Relationship between specifically expressed gene (SEG) annotations and background selection statistic (BSS).** a) Correlation between 53 SEG annotations and BSS. Tissues are ranked by magnitude of correlation. **a)** Mean BSS at annotated SNPs for 53 SEG annotations. Tissues are ranked by magnitude of the mean.



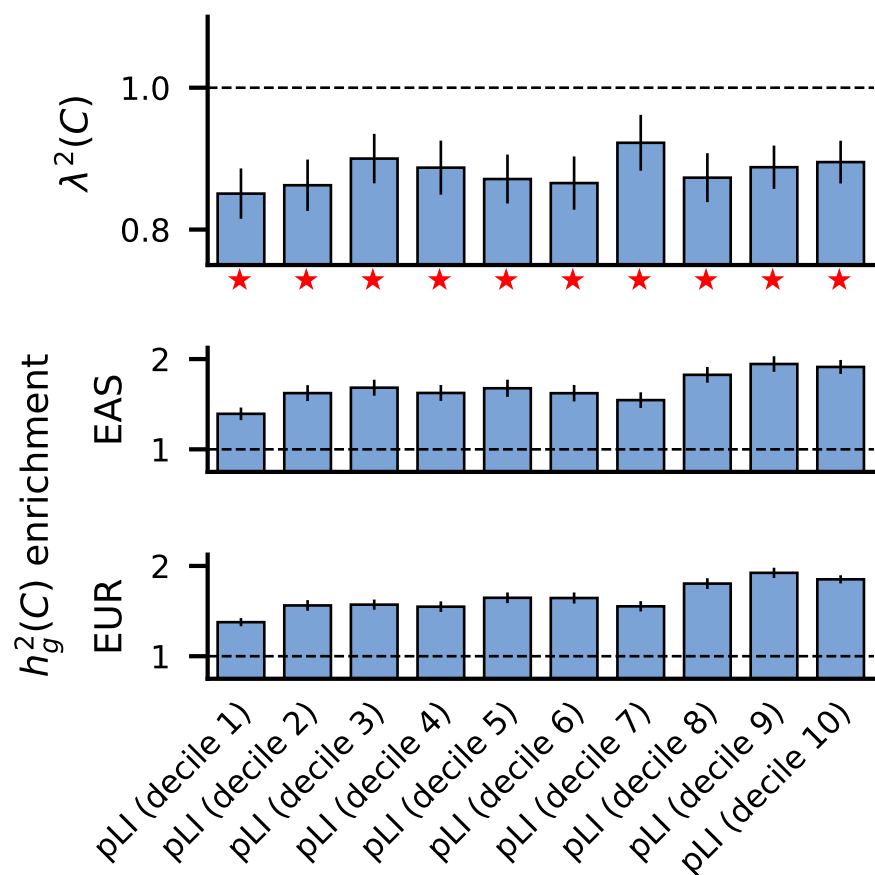
Supplementary Figure 27: **Relationship between specifically expressed gene (SEG) annotations and CpG content.** a) Correlation between 53 SEG annotations and CpG content. Tissues are ranked by magnitude of correlation. a) Mean CpG content at annotated SNPs for 53 SEG annotations. Tissues are ranked by magnitude of the mean.



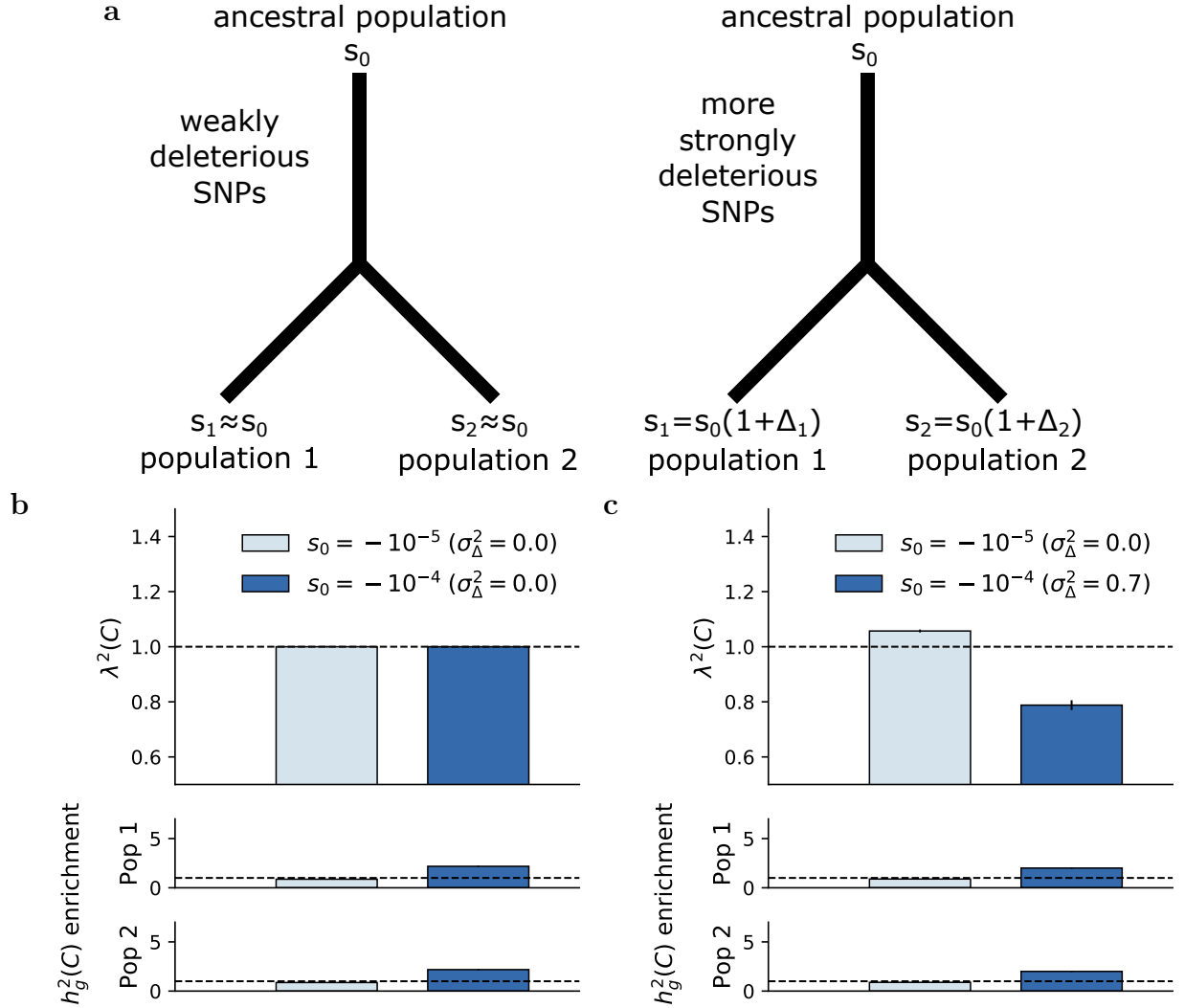
Supplementary Figure 28: **Correlation between specifically expressed gene annotations and 8 continuous-valued annotations.** Annotations are sorted inversely based on their correlation with background selection statistic.



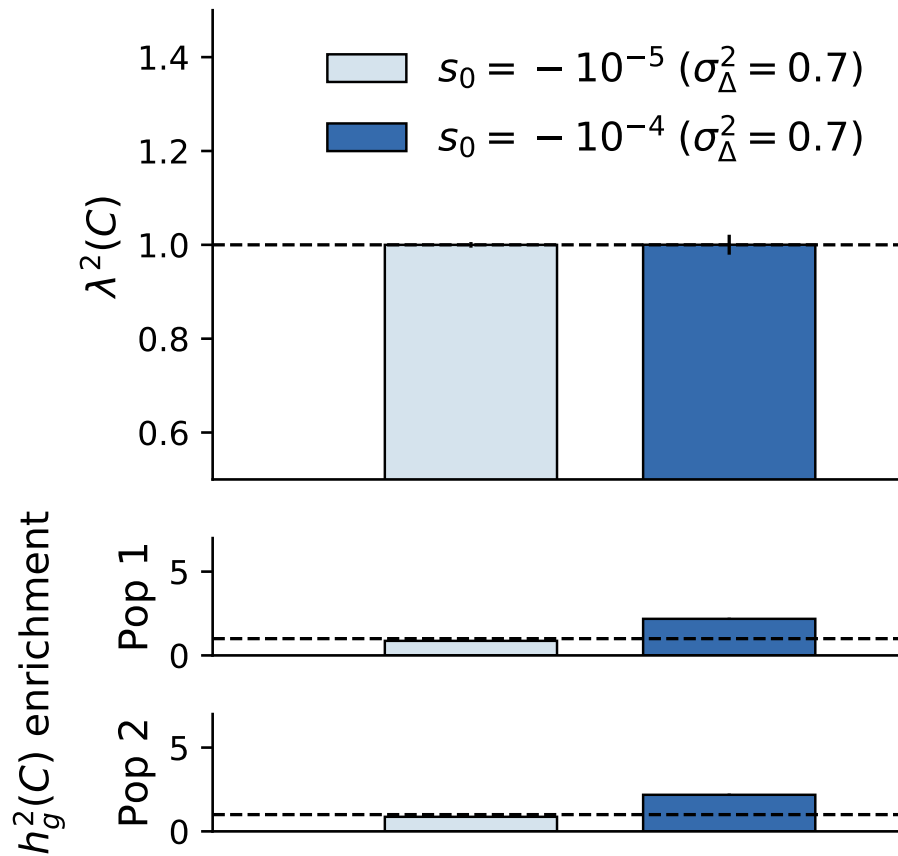
Supplementary Figure 29: **Correlation between probability of loss-of-function intolerance (pLI) decile gene annotations and 8 continuous-valued annotations.** Here, correlations are calculated across all SNPs with minor allele frequency greater than 5% in both East Asian and European populations.



Supplementary Figure 30: **S-LDXR** results for deciles of probability of loss-of-function intolerance (pLI) annotations across 31 diseases and complex traits. Deciles with  $\lambda^2(C)$  significantly less than 1 are marked by red stars. Numerical results can be found in Supplementary Table 5. Error bars denote  $\pm 1.96 \times$  standard errors of the meta-analyzed  $\lambda^2(C)$ . P-values are obtained from a standard normal distribution. Red stars ( $\star$ ) denote two-tailed  $p < 0.05/10$ .



Supplementary Figure 31: **Evolutionary modeling results using 2-population extension of Eyre-Walker model.** We use negative  $s$  to denote deleteriousness, following convention of previous works.<sup>11,12</sup> However, positive  $s$  (i.e. beneficial mutations) may also be plausible. (a) Diagrams illustrating fitness effects in population 1 and population 2 ( $s_1$  and  $s_2$ ) as a function of the fitness effect in the ancestral population ( $s_0$ ) at weakly deleterious SNPs (left; e.g. corresponding to SNPs in bottom quintile of background selection statistic) and more strongly deleterious SNPs (right; e.g. corresponding to SNPs in top quintile of background selection statistic). (b), (c) We report enrichment/depletion of squared trans-ethnic genetic correlation ( $\lambda^2(C)$ ) for SNPs with different fitness effects, in simulations under a two-population extension of the Eyre-Walker model with (b)  $\sigma_\Delta^2 = 0$  for both weakly deleterious SNPs ( $s_0 = -10^{-5}$ ) and more strongly deleterious SNPs ( $s_0 = -10^{-4}$ ), (c)  $\sigma_\Delta^2 = 0.0$  for weakly deleterious SNPs and  $\sigma_\Delta^2 = 0.7$  for more strongly deleterious SNPs. Results are averaged across 1,000 simulations. Error bars denote  $\pm 1.96 \times$  standard error of the mean. Numerical results are reported in Supplementary Table 6.



Supplementary Figure 32: **Evolutionary modeling results using 2-population extension of Eyre-Walker model with  $\sigma_{\Delta}^2 = 0.7$  for both weakly deleterious and more strongly deleterious SNPs.** We use negative  $s$  to denote deleteriousness, following convention of previous works.<sup>11,12</sup> However, positive  $s$  (i.e. beneficial mutations) may also be plausible. We report enrichment/depletion of squared trans-ethnic genetic correlation ( $\lambda^2(C)$ ) for SNPs with different fitness effects, in simulations under a two-population extension of the Eyre-Walker model,<sup>10</sup> with  $\sigma_{\Delta}^2 = 0.7$  for both weakly deleterious and more strongly deleterious SNPs. Results are averaged across 1,000 simulations. Error bars denote  $\pm 1.96 \times$  standard error of the mean.



## 219 Supplementary References

## 220 References

- 221 [1] Kevin J Galinsky et al. “Estimating cross-population genetic correlations of causal  
222 effect sizes”. In: *Genetic epidemiology* 43.2 (2019), pp. 180–188.
- 223 [2] Brielin C Brown et al. “Transethnic genetic-correlation estimates from summary  
224 statistics”. In: *The American Journal of Human Genetics* 99.1 (2016), pp. 76–88.
- 225 [3] Hilary K Finucane et al. “Partitioning heritability by functional annotation using  
226 genome-wide association summary statistics”. In: *Nature genetics* 47.11 (2015), p. 1228.
- 227 [4] 1000 Genomes Project Consortium et al. “A global reference for human genetic vari-  
228 ation”. In: *Nature* 526.7571 (2015), p. 68.
- 229 [5] Leon Isserlis. “On a formula for the product-moment coefficient of any order of a  
230 normal frequency distribution in any number of variables”. In: *Biometrika* 12.1/2  
231 (1918), pp. 134–139.
- 232 [6] Brendan K Bulik-Sullivan et al. “LD Score regression distinguishes confounding from  
233 polygenicity in genome-wide association studies”. In: *Nature genetics* 47.3 (2015),  
234 p. 291.
- 235 [7] Brendan Bulik-Sullivan et al. “An atlas of genetic correlations across human diseases  
236 and traits”. In: *Nature genetics* 47.11 (2015), p. 1236.
- 237 [8] International HapMap 3 Consortium et al. “Integrating common and rare genetic  
238 variation in diverse human populations”. In: *Nature* 467.7311 (2010), p. 52.
- 239 [9] James Durbin. “A note on the application of Quenouille’s method of bias reduction  
240 to the estimation of ratios”. In: *Biometrika* 46.3/4 (1959), pp. 477–480.
- 241 [10] Adam Eyre-Walker. “Genetic architecture of a complex trait and its implications for  
242 fitness and genome-wide association studies”. In: *Proceedings of the National Academy  
243 of Sciences* (2010), p. 200906182.
- 244 [11] Steven Gazal et al. “Linkage disequilibrium–dependent architecture of human complex  
245 traits shows action of negative selection”. In: *Nature genetics* 49.10 (2017), p. 1421.
- 246 [12] S Gazal et al. “Functional architecture of low-frequency variants highlights strength  
247 of negative selection across coding and non-coding annotations.” In: *Nature genetics*  
248 50.11 (2018), p. 1600.
- 249 [13] Arun Durvasula and Kirk E Lohmueller. “Negative selection on complex traits limits  
250 genetic risk prediction accuracy between populations”. In: *bioRxiv* (2019), p. 721936.

- 251 [14] Armando Caballero, Albert Tenesa, and Peter D Keightley. “The nature of genetic  
252 variation for complex traits revealed by GWAS and regional heritability mapping  
253 analyses”. In: *Genetics* 201.4 (2015), pp. 1601–1613.
- 254 [15] Yuval B Simons et al. “A population genetic interpretation of GWAS findings for  
255 human quantitative traits”. In: *PLoS biology* 16.3 (2018), e2002985.
- 256 [16] Siew-Kee Low et al. “Identification of six new genetic loci associated with atrial  
257 fibrillation in the Japanese population”. In: *Nature genetics* 49.6 (2017), p. 953.
- 258 [17] Jonas B Nielsen et al. “Biobank-driven genomic discovery yields new insight into  
259 atrial fibrillation biology”. In: *Nature genetics* 50.9 (2018), p. 1234.
- 260 [18] Momoko Horikoshi et al. “Elucidating the genetic architecture of reproductive ageing  
261 in the Japanese population”. In: *Nature communications* 9.1 (2018), p. 1977.
- 262 [19] Felix R Day et al. “Large-scale genomic analyses link reproductive aging to hypothalamic signaling, breast cancer susceptibility and BRCA1-mediated DNA repair”. In:  
263 *Nature genetics* 47.11 (2015), p. 1294.
- 264 [20] Masahiro Kanai et al. “Genetic analysis of quantitative traits in the Japanese popu-  
265 lation links cell types to complex human diseases”. In: *Nature genetics* 50.3 (2018),  
266 p. 390.
- 267 [21] William J Astle et al. “The allelic landscape of human blood cell trait variation and  
268 links to common complex disease”. In: *Cell* 167.5 (2016), pp. 1415–1429.
- 269 [22] Po-Ru Loh et al. “Mixed-model association for biobank-scale datasets”. In: *Nature*  
270 *genetics* 50.7 (2018), p. 906.
- 271 [23] Cristian Pattaro et al. “Genetic associations at 53 loci highlight cell types and bio-  
272 logical pathways relevant for kidney function”. In: *Nature communications* 7 (2016),  
273 p. 10023.
- 274 [24] Masato Akiyama et al. “Characterizing rare and low-frequency height-associated vari-  
275 ants in the Japanese population”. In: *Nature Communications* 10.1 (2019), pp. 1–11.
- 276 [25] Na Cai et al. “Sparse whole-genome sequencing identifies two loci for major depressive  
277 disorder”. In: *Nature* 523.7562 (2015), p. 588.
- 278 [26] Naomi R Wray et al. “Genome-wide association analyses identify 44 risk variants and  
279 refine the genetic architecture of major depression”. In: *Nature genetics* 50.5 (2018),  
280 p. 668.
- 281 [27] Yukinori Okada et al. “Genetics of rheumatoid arthritis contributes to biology and  
282 drug discovery”. In: *Nature* 506.7488 (2014), p. 376.
- 283 [28] Max Lam et al. “Comparative genetic architectures of schizophrenia in East Asian  
284 and European populations”. In: *Nature genetics* 51.12 (2019), pp. 1670–1678.
- 285

- 286 [29] Ken Suzuki et al. “Identification of 28 new susceptibility loci for type 2 diabetes in  
287 the Japanese population”. In: *Nature genetics* 51.3 (2019), p. 379.
- 288 [30] Robert A Scott et al. “An expanded genome-wide association study of type 2 diabetes  
289 in Europeans”. In: *Diabetes* 66.11 (2017), pp. 2888–2902.
- 290 [31] Margaux LA Hujoel et al. “Combining case-control status and family history of disease  
291 increases association power”. In: *bioRxiv* (2019), p. 722645.
- 292 [32] Clare Bycroft et al. “The UK Biobank resource with deep phenotyping and genomic  
293 data”. In: *Nature* 562.7726 (2018), p. 203.
- 294 [33] Jason C Simeone et al. “An evaluation of variation in published estimates of schizophre-  
295 nia prevalence from 1990–2013: a systematic literature review”. In: *BMC psychiatry*  
296 15.1 (2015), p. 193.